TAMUK: 0-5516

Wave Forces on Bridge Decks: State of the Art and State of the Practice Review

Technical Report 0-5516-1

Cooperative Research Program

TEXAS A&M UNIVERSITY–KINGSVILLE
KINGSVILLE, TEXAS

TEXAS DEPARTMENT OF TRANSPORTATION

in cooperation with the
Federal Highway Administration and the
Texas Department of Transportation
http://users.tamuk.edu/kfgfa00/Wave%20Loads.HTM

Technical Report Documentation Page

1. Report No.	2. Government Accession No.	3. Recipient's Catalog No.
FHWA/TX-08/0-5516-1		

4. Title and Subtitle	5. Report Date
WAVE FORCES ON BRIDGE DECKS: STATE OF THE ART AND STATE OF THE PRACTICE REVIEW	October 2006 Published: February 2008
	6. Performing Organization Code
7. Author(s) Francisco Aguíñiga, Kevin Matakis, Hector Estrada, Joseph Sai, Pat Leelani, and Jeff Shelden	8. Performing Organization Report No. Report 0-5516-1
9. Performing Organization Name and Address Texas A&M University-Kingsville 700 University Blvd., MSC 194 Kingsville, Texas 78363	10. Work Unit No. (TRAIS) 11. Contract or Grant No. Project 0-5516
12. Sponsoring Agency Name and Address Texas Department of Transportation Research and Technology Implementation Office P. O. Box 5080 Austin Texas 78763-5080	13. Type of Report and Period Covered Technical Report: September 2005 – August 2006 14. Sponsoring Agency Code

15. Supplementary Notes

Project conducted in cooperation with the Texas Department of Transportation and the Federal Highway Administration.

Project Title: Synthesis of Wave Load Design Methods for Coastal Bridges

URL: http://users.tamuk.edu/kfgfa00/Wave%20Loads.HTM

16. Abstract

The extensive bridge damage caused by recent hurricanes on the Gulf of Mexico showed a need for a design method against wave forces. A literature review revealed that current guidelines offer limited help to bridge designers, since current information related to the design of bridge superstructures when subjected to the action of waves is inadequate. This document presents a compilation of available sources of information that contain information related to forces produced by waves acting on engineering structures such as sea walls, suspended walls, and bridge decks.

17. Key Words	18. Distribution Statement
Bridge, Wave, Period, Height, Sea, Significant, Hurricane, Design, Force, Impact, Hydrostatic	No restrictions. This document is available to the public through NTIS: National Technical Information Service 5285 Port Royal Road Springfield, Virginia 22161

19. Security Classif.(of this report)	20. Security Classif.(of this page)	21. No. of Pages	22. Price
Unclassified	Unclassified	96	

WAVE FORCES ON BRIDGE DECKS: STATE OF THE ART AND STATE OF THE PRACTICE REVIEW

by

Francisco Aguíñiga
Assistant Professor
Texas A&M University-Kingsville

Kevin Matakis
Research Assistant
Texas A&M University-Kingsville

Hector Estrada
Professor
University of the Pacific

Joseph Sai
Professor
Texas A&M University-Kingsville

Pat Leelani
Professor
Texas A&M University-Kingsville

and

Jeff Shelden
Consulting Engineer
Moffatt and Nichol Engineers

Report 0-5516-1
Project 0-5516
Project Title: Synthesis of Wave Load Design Methods for Coastal Bridges

Performed in cooperation with the
Texas Department of Transportation
and the
Federal Highway Administration

February 2008

TEXAS A&M UNIVERSITY-KINGSVILLE
Department of Civil and Architectural Engineering
700 University Blvd., MSC 194
Kingsville, Texas 78363

DISCLAIMER

The contents of this report reflect the views of the authors, who are responsible for the facts and the accuracy of the data presented herein. The contents do not necessarily reflect the official view or policies of the Texas Department of Transportation or the Federal Highway Administration. This report does not constitute a standard, specification, or regulation.

ACKNOWLEDGMENTS

Research performed in cooperation with the Texas Department of Transportation and the Federal Highway Administration.

The authors wish to express their gratitude to:

Program Coordinator:
Gary K. Trietsch, P.E., Texas Department of Transportation, Houston District

Project Director (with special thanks for his continued support and input):
Jon Holt, P.E., Texas Department of Transportation, Houston District

Project Advisors:
George Herrmann, P.E., Texas Department of Transportation, Houston District
Rose Marie Klee, E.I.T., Texas Department of Transportation, Design Division
Michelle Romage, P.E., Texas Department of Transportation, Bridge Division
Amy Ronnfeldt, P.E., Texas Department of Transportation, Design Division

The first author wishes to acknowledge and thank God's help on this project.

TABLE OF CONTENTS

Page

TABLE OF CONTENTS (CONT.)

LIST OF FIGURES

FIGURE Page

LIST OF FIGURES (CONT.)

FIGURE Page

LIST OF TABLES

TABLE Page

I. INTRODUCTION

In recent decades, oil platforms have experienced damage or failure due to waves produced by hurricanes (Bea et al., 1999). For this reason, the design of offshore platforms for the oil industry has devoted considerable effort to study the effects of wave loads on offshore platform decks. Due to population growth on coastal areas of the Atlantic and Gulf of Mexico, wave loads have become a problem for highway bridges. The bridges on U.S. HW 90 across Biloxi Bay and St. Louis Bay were heavily damaged by hurricane Camille in 1969 (Denson, 1980). In 2004, hurricane Ivan overturned several spans of the Escambia Bay Bridge in Florida. Shortly after this research began, hurricane Katrina severely damaged the bridge on U.S. HW 90 across St. Louis Bay, MS, the bridge on U.S. HW 90 across Biloxi Bay, MS, and the bridge on I-10 across Lake Pontchartrain in New Orleans, LA. Hurricane Katrina by itself caused the largest natural disaster in U.S. history, resulting in 1800 lives lost and billions of dollars in property damage. A preliminary review of the existing design codes and guidelines for the design of bridge decks subjected to wave loads revealed that there is limited information available. This indicates the need to carry out a literature search that summarizes design methods that could potentially be used to estimate wave forces on bridge decks. This research report will provide a description of literature related to available methods for the design of structures subjected to sea waves. Literature available in design codes, documents that contain information that could be used to estimate wave forces on bridge decks, and sources of information for wave forces on bridge substructures and bridge revetments are given.

II. DESIGN METHODS

This chapter describes the methods currently available in the literature for the design of bridges to sustain wave forces. The information is focused on bridge superstructures. Information on design guidelines or government documents related to bridge superstructure design is presented first. Information about wave loads on bridge superstructures or similar elements that includes summaries of journal articles, books, chapters, and research reports is also included in this section. This chapter ends with sections on guidelines and information about the design of bridge substructures and bridge revetments.

DESIGN GUIDELINES FOR WAVE FORCES ON BRIDGE SUPERSTRUCTURE

Current bridge design codes appear to provide limited guidance for the design of bridge superstructures subjected to storm wave and surge forces. Many books and design aids are currently available for bridge designers (AASHTO, 2004; CALTRANS, 2005a, b, c; Chen and Duan, 1999; Taly, 1998; TxDOT, 1997; TxDOT, 2001; Xhantakos, 1994; ASCE/SEI24-05, 2006; ASCE/SEI7-05, 2006; FEMA, 2000; CEM, 2006). The design of bridge superstructures spanning a body of water typically does not account for water flow forces. A description of current design aids and specifications as they impact the design of bridge superstructures subjected to water flow forces is given next.

A number of references indicate that during a bridge design it seems that they all imply that the bridge type is selected to safely accommodate any flow underneath the superstructure (AASHTO, 2004; CALTRANS, 2005b; Chen and Duan, 1999; Taly, 1998; TxDOT, 1997; Xhantakos, 1994).

California Department of Transportation – Bridge Design – 2005

The maximum water level expected to occur during the design life of the bridge is estimated, and the height of the superstructure above the maximum water level is selected (CALTRANS, 2005b). This height is typically greater than 6 ft (CALTRANS 2005a). That is, bridge superstructures are typically not designed to sustain flow forces derived from storm surge. In this regard, the Bridge Design Specifications of the California Department of Transportation indicate that: "In cases where the corresponding top of water elevation is above the low beam elevation, stream flow loading on the superstructure shall be investigated" (CALTRANS, 2005c). However, the specifications indicate that "The stream flow pressure acting on the superstructure may be taken as P_{max} with a uniform distribution," (CALTRANS, 2005c). The pressure P_{max} is equal to twice the pressure P_{avg}, where P_{avg} is computed with the following expression:

$$P_{avg} = K\left(V_{avg}\right)^2 \qquad \text{Equation 1}$$

where,

P_{avg} = average stream pressure, in pounds per square foot

V_{avg} = average velocity of water in feet per second; computed by dividing the flow rate by the flow area

K = a constant, being 1.4 for all piers subjected to drift build-up and square-ended piers, 0.7 for circular piers, and 0.5 for angle-ended piers where the angle is 30 degrees or less

Taly and Xanthakos do not mention water flow forces for the design of bridge superstructures (Taly, 1998; Xanthakos, 1994).

Section 1.10 of the Bridge Design Practice Manual of the California Department of Transportation recommends the use of box girders or slabs for bridge superstructures where less than 6 feet of clearance is provided over a stream carrying drift (CALTRANS, 2005a).

AASHTO – LRFD Bridge Design Specifications – 2004

The American Association of State Highway and Transportation Officials (AASHTO) LRFD Bridge Design Specifications contain no recommendations for superstructure design against water flow forces (AASHTO, 2004). Section 3.7.4 of the AASHTO Bridge Design Specifications recommends the use of the Shore Protection Manual to account for wave loads in the design of bridge structures, although it does not specifically address superstructures. The commentary of Section 2.6.4.3 of the AASHTO Bridge Design Specifications indicates that trial combinations for the size of a bridge should take into account the clearances between the floodwater elevations and low sections of the superstructure to allow passage of ice and debris. Section 2.3.1.2 of the AASHTO Bridge Design Specifications also indicates that: "It is generally safer and more cost effective to avoid hydraulic problems through the selection of favorable crossing locations than to attempt to minimize the problems at a later time in the project development process through design measures."

TxDOT – Hydraulic Design Manual – 1997

Section 8.11.6 Minimizing Hydraulic Forces and Debris Impact on the Superstructure of the Hydraulic Design Manual published by the Texas Department of Transportation states that (TxDOT, 1997): "The most obvious design objective is to avoid the imposition of hydraulic forces on a bridge superstructure by placing the bridge at an elevation above which the probability of submergence is small." The manual also indicates that: "Where there is even a small probability of total or partial submergence, the designer should ensure that there is minimum potential for the bridge deck to float away. If the dead load of the structure' (superstructure) 'is not sufficient to resist buoyant, drag, and debris impact forces, it will be necessary to anchor the superstructure to the substructure. Air holes should also be provided through each span and between each girder to reduce the uplift pressure."

In a previous section it is mentioned that the Bridge Design Practice Manual of CALTRANS recommends the use of box girders or slabs for bridge superstructures (CALTRANS, 2005a). However, Section 8.11.6 of the Hydraulic Design Manual of TxDOT makes the opposite recommendation: "Box girders which would displace great volumes of water and have a relatively small weight compared to the weight of the water displaced are not a good design alternative unless the probability of submergence is small."

Bridges located in a coastal area where hurricanes are recurring events need to be designed for such events. As mentioned in the bridge superstructure section, the best approach is to avoid having the superstructure coming in contact with the flow of water for the extreme flood event. However, as mentioned in Ssection 8.11.6 of the Hydraulic Design Manual of TxDOT, that is not always physically feasible. During a hurricane, the bridge superstructure may be subjected not only to water flow forces, but to vessel or debris collision as well.

U.S. Army Corps of Engineers – Coastal Engineering Manual – 2006

The Coastal Engineering Manual (CEM) is one of the most widely used sources for the design of coastal structures in the U. S. The manual is a good source of information to obtain data on wave theories and design methods for different coastal structures. The part of the manual most closely related to wave forces on a bridge deck is found under Part VI Introduction to Coastal Project Element Design, Chapter 5, Fundamentals of Design, Section VI-5-4 Vertical-Front Structure Loading and Response. This section of the manual indicates that the pressures generated by waves on the structures are difficult to obtain with certainty and are a function of the wave conditions and structure geometry. The manual recommends the formulae presented in that section to be used only for preliminary design, accounting for the limitations of each parameter and all uncertainties. They also recommend the final design of an important structure to include laboratory tests. The manual identifies three different wave types affecting vertical walls: non-breaking waves, breaking waves with almost vertical fronts, and breaking waves with large air pockets. It is mentioned that there are no reliable formulae for prediction of impulsive pressures produced by breaking waves due to the extremely stochastic nature of wave impacts. The impulsive loads produced by breaking waves can be quite large, and the extreme load risk increases with the number of breaking waves. Frequent wave breaking is not expected on vertical structures with an angle of wave incidence larger than 20° from the normal incidence. The slope of the seabed also influences the effect of breaking waves. Mild slopes of approximately 1:50 or less over a distance of several wave lengths are not likely to make waves break on the structure.

The CEM indicates that the total hydrodynamic pressure distribution on a vertical wall has two components: the hydrostatic pressure produced by the instantaneous water depth at the wall, and a dynamic component due to the water particle accelerations. The pressure equations used by the manual on vertical walls are mainly based on the equations derived by Goda and modified by others to design for a variety of conditions (Goda, 1974). The equations given in the CEM are shown in Figures 1, 2, and 3. A summary of a book written by Goda is given under the section of relevant literature about wave forces on bridge superstructures.

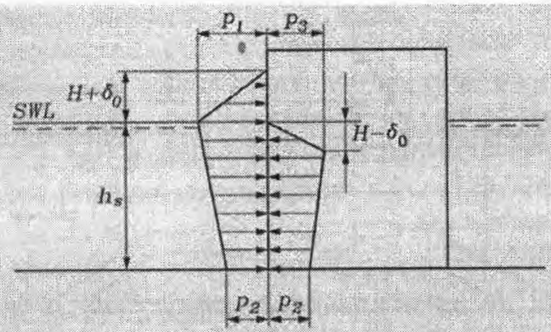

$$p_1 = (p_2 + \rho_w g h_s)\frac{H + \delta_o}{h_s + H + \delta_o}$$

$$p_2 = \frac{\rho_w g H}{\cosh(2\pi h_s/L)}$$

$$p_3 = \rho_w g(H - \delta_o)$$

$$\delta_o = \frac{\pi H^2}{L}\coth\frac{2\pi h_s}{L}$$

where H = Wave height. In case of irregular waves, H should be taken as a characteristic wave height. In Japan $H_{1/3}$ is used, while in other countries $H_{1/10}$ might be used.

p_1 = Wave pressure at the still water level, corresponding to wave crest

p_2 = Wave pressure at the base of the vertical wall

p_3 = Wave pressure at the still water level, corresponding to wave trough

δ_o = Vertical shift in the wave crest and wave trough at the wall

ρ_w = Water density

h_s = Water depth at the foot of the structure

L = Local wave length.

Remarks. The Sainflou formula for conditions under wave crest and wave trough were derived theoretically for the case of regular waves and a vertical wall. The formula cannot be applied in cases where wave breaking and/or overtopping takes place.

Figure 1. The Sainflou formula for head-on, fully reflected, standing regular waves, modified from: (CEM, 2006).

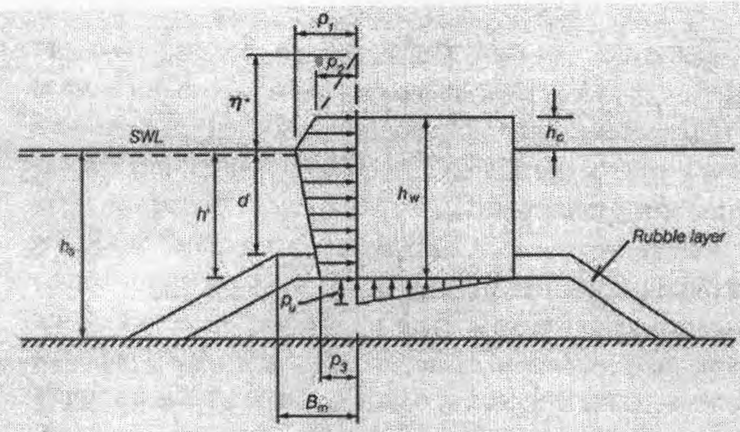

$$
\begin{aligned}
\eta^* &= 0.75(1+cos\beta)\,\lambda_1 H_{design} \\
p_1 &= 0.5(1+cos\beta)(\lambda_1\alpha_1+\lambda_2\alpha_* cos^2\beta)\,\rho_w\, g\, H_{design} \\
p_2 &= \begin{cases} \left(1-\frac{h_c}{\eta^*}\right)p_1 & \text{for } \eta^* > h_c \\ 0 & \text{for } \eta^* \le h_c \end{cases} \\
p_3 &= \alpha_3\, p_1 \\
p_u &= 0.5(1+cos\beta)\lambda_3\alpha_1\alpha_3\rho_w g\, H_{design}
\end{aligned}
$$

where

β = Angle of incidence of waves (angle between wave crest and front of structure)

H_{design} Design wave height defined as the highest wave in the design sea state at a location just in front of the breakwater. If seaward of a surf zone Goda (1985) recommends for practical design a value of 1.8 H_s to be used corresponding to the 0.15% exceedence value for Rayleigh distributed wave heights. This corresponds to $H_{1/250}$ (mean of the heights of the waves included in 1/250 of the total number of waves, counted in descending order of height from the highest wave). Goda's recommendation includes a safety factor in terms of positive bias as discussed in Table VI-5-55. If within the surf zone, H_{design} is taken as the highest of the random breaking waves at a distance $5H_s$ seaward of the structure.

$$
\begin{aligned}
\alpha_* &= \alpha_2 \\
\alpha_1 &= 0.6+0.5\left[\frac{4\pi h_s/L}{sinh\,(4\pi h_s/L)}\right]^2 \\
\alpha_2 &= \text{the smallest of } \frac{h_b-d}{3\,h_b}\left(\frac{H_{design}}{d}\right)^2 \text{ and } \frac{2d}{H_{design}} \\
\alpha_3 &= 1-\frac{h_w-h_c}{h_s}\left[1-\frac{1}{cosh\,(2\pi h_s/L)}\right]
\end{aligned}
$$

L = Wavelength at water depth h_b corresponding to that of the significant wave $T_s \simeq 1.1T_m$, where T_m is the average period.

h_b = Water depth at a distance of $5H_s$ seaward of the breakwater front wall.

λ_1, λ_2 and λ_3 are modification factors depending on the structure type. For conventional vertical wall structures, $\lambda_1 = \lambda_2 = \lambda_3 = 1$. Values for other structure types are given in related tables.

Figure 2. Goda formula for irregular waves, modified from: (CEM, 2006).

The modification of Goda's formula concerns the formula for the pressure p_1 at the still water level (SWL). The coefficient α_* is modified as

$$\alpha_* = \text{largest of } \alpha_2 \text{ and } \alpha_I$$

$$\alpha_2 = \text{the smallest of } \frac{h_b - d}{3h_b}\left(\frac{H_{design}}{d}\right)^2 \text{ and } \frac{2d}{H_{design}}$$

$$\alpha_I = \alpha_{I0} \cdot \alpha_{I1}$$

$$\alpha_{I0} = \begin{cases} H_{design}/d & \text{for } H_{design}/d \leq 2 \\ 2.0 & \text{for } H_{design}/d > 2 \end{cases}$$

$$\alpha_{I1} = \begin{cases} \frac{\cos\delta_2}{\cosh\delta_1} & \delta_2 \leq 0 \\ \frac{1}{\cosh\delta_1 \cdot (\cosh\delta_2)^{\frac{1}{2}}} & \delta_2 > 0 \end{cases}$$

$$\delta_1 = \begin{cases} 20 \cdot \delta_{11} & \text{for } \delta_{11} \leq 0 \\ 15 \cdot \delta_{11} & \text{for } \delta_{11} > 0 \end{cases}$$

$$\delta_{11} = 0.93\left(\frac{B_m}{L} - 0.12\right) + 0.36\left(\frac{h_s - d}{h_s} - 0.6\right)$$

$$\delta_2 = \begin{cases} 4.9 \cdot \delta_{22} & \text{for } \delta_{22} \leq 0 \\ 3 \cdot \delta_{22} & \text{for } \delta_{22} > 0 \end{cases}$$

$$\delta_{22} = -0.36\left(\frac{B_m}{L} - 0.12\right) + 0.93\left(\frac{h_s - d}{h_s} - 0.6\right)$$

where H_{design}, L, d, h_s, h_b, B_m are given in the figure and text of Table VI-5-53.

Range of tested parameters:	Regular waves	
	bottom slope 0.01	h_s = 42 cm and 54 cm
	d = 7 - 39 cm	B_m = 2.5 - 200 cm
	H = 17.2 - 37.8 cm	T - 1.8 - 3 sec.

Figure 3. Goda formula modified to include impulsive forces from head-on breaking waves, source: (CEM, 2006).

The older breaking wave force method proposed by Minikin (Minikin, 1950) used in the Shore Protection Manual (SPM, 1984) is not included in the Coastal Engineering Manual. It is considered that the Minikin method can result in estimates of wave forces, as high as 15 to 18 times those calculated for non-breaking waves. As such, the Minikin method is deemed overconservative.

ASCE/SEI 24-05 – Flood Resistant Design and Construction – 2006

This ASCE standard (ASCE/SEI 24-05, 2006) does not contain wave design forces per se. However, it addresses the subject of wave loads on structures. The standard uses the following relevant definitions among others:

Base Flood Elevation (BFE) – elevation of flooding, including wave height, having a 1% chance of being equalled or exceeded in any given year.
Base Flood – flood having a 1% chance of being equalled or exceeded in any given year.
Design Flood – greater of the following two flood events: (1) the *base flood*, affecting those areas identified as *special flood hazard areas* on the community's Flood Insurance Rate Map (FIRM); or (2) the flood corresponding to the area designated as flood hazard area on a community's *flood hazard map* or otherwise legally designated.
Design Flood Elevation (DFE) – elevation of the *design flood*, including wave height, relative to the datum specified on the community's *flood hazard map*.
High Velocity Wave Action – condition where wave heights are greater than or equal to 3.0 ft in height or where wave runup elevations reach 3.0 ft or more above grade.

The standards classify structures in different categories. Essential facilities such as causeways would fit in category IV, which is the highest rank.

The standards mentioned in Section 4.8, that decks, concrete pads, and patios shall not transfer flood loads to the main structure. It indicates that they should be designed to break away cleanly during design flood conditions. The standards also indicate in Table 5-1 that the minimum elevation relative to the base flood elevation for a type IV structure shall be the greater of the base flood elevation plus 2 ft or the design flood elevation. Regarding wind generated waves the standard recommends to use the Shore Protection Manual – now called Coastal Engineering Manual (CEM, 2006) and a document published by the National Academy of Sciences (National Academy of Sciences, 1977) if waves greater than 3 ft can develop at the site.

ASCE/SEI 7-05 – Minimum Design Loads for Buildings and Other Structures – 2006

This standard addresses loads on structures due to flooding in Chapter 5 (ASCE/SEI 7-05, 2006). This standard has the design requirement that structural systems or buildings be designed, constructed, connected and anchored to resist flotation, permanent lateral displacement due to flood loads, and collapse.

Wave loads are to be determined by: the methods given in the standard, advanced numerical modelling procedures, or by laboratory test procedures.

Buildings shall be designed for the following loads: waves breaking on any portion of the building or structure, uplift forces caused by shoaling underneath a structure, wave runup striking any portion of the building, and wave-induced scour.

Non-breaking waves

In this case the structure shall be designed for hydrostatic and hydrodynamic loads. A detailed analysis should be carried out to determine the dynamic effects of moving water. When water velocities do not exceed 10 ft/sec it is permitted to account for the dynamic effects by using an equivalent hydrostatic load. Thus, the design flood elevation (DFE) should be increased by a depth d_h on the headwater side equal to:

$$d_h = \frac{aV^2}{2g} \qquad \text{Equation 2}$$

where,

V = average velocity of water, *ft/s*

g = acceleration of gravity, 32.2 ft/s^2

a = coefficient of drag or shape factor (not less than 1.25)

Breaking wave loads on rigid vertical pilings and columns

Breaking wave height shall be computed as:

$$H_b = 0.78 d_s \qquad \text{Equation 3}$$

where,

H_b = Breaking wave height, *ft*

d_s = Local still water depth, *ft*

Unless more advanced studies are used, local still water depth can be computed using:

$$d_s = 0.65(BFE - G) \qquad \text{Equation 4}$$

where,

BFE = Base flood elevation, *ft*

G = Ground elevation, *ft*

The net force produced by a breaking wave shall be assumed to act at the still water elevation and shall be computed by:

$$F_D = 0.5 \gamma_w C_D D H_b^2 \qquad \text{Equation 5}$$

where,

F_D = Net wave force, lb

γ_w = Unit weight of water, 62.4 lb/ft^3 for fresh water and 64 lb/ft^3 for salt water

C_D = Drag coefficient for breaking waves = 1.75 for circular piles or columns, and = 2.25 for square piles or columns

D = Pile or column diameter, 1.4 times width of square pile or column, *ft*

Breaking wave loads on vertical walls

The maximum pressures and net forces produced by a normally incident wave (depth limited in size, with $H_b = 0.78 d_s$) breaking on a rigid vertical wall shall be calculated by:

$$P_{\max} = C_p \gamma_w d_s + 1.2 \gamma_w d_s \qquad \text{Equation 6}$$

and

$$F_t = 1.1 C_p \gamma_w d_s^2 + 2.4 \gamma_w d_s^2 \qquad \text{Equation 7}$$

where,

P_{max} = Maximum combined dynamic ($C_p \gamma_w d_s$) and static ($1.2 \gamma_w d_s$) wave pressures, also known as shock pressures, *lb/ft*^{2}

F_t = Net breaking wave force per unit length of structure, also known as shock, impulse, or wave impact force, developed near the still water elevation, *lb/ft*

C_p = Dynamic pressure coefficient (varies from 1.6 for temporary facilities to 3.5 for essential facilities)

d_s = Still water depth at base of building or structure where the wave breaks, *ft*

This procedure assumes the vertical wall reflects the wave to a height of $1.2d_s$ as shown in Figure 4, and that the space behind the vertical wall is dry.

When there is water behind the wall the maximum combined pressure is given by Equation 6 and the net force shall be computed by:

$$F_t = 1.1 C_p \gamma_w d_s^2 + 1.9 \gamma_w d_s^2 \qquad \text{Equation 8}$$

where all the terms are as described before. This loading case is depicted in Figure 5.

The ASCE/SEI 7-05 document also contains some recommendations for breaking wave loads on non-vertical walls. The standards indicate the horizontal component of the breaking wave force is given by:

$$F_{nv} = F_t \sin^2 \alpha \qquad \text{Equation 9}$$

where,

F_{nv} = Horizontal component of breaking wave force, *lb/ft*

F_t = Net breaking wave force acting on a vertical surface, *lb/ft*

α = Vertical angle between non-vertical surface and the horizontal

The document also presents an expression to compute the load produced by an obliquely incident breaking wave:

$$F_{oi} = F_t \sin^2 \alpha \qquad \text{Equation 10}$$

where,

F_{oi} = Horizontal component of obliquely incident breaking wave force, *lb/ft*

F_t = Net breaking wave force (from normally incident waves) acting on a vertical surface, *lb/ft*

α = Horizontal angle between the direction of wave approach and the vertical surface

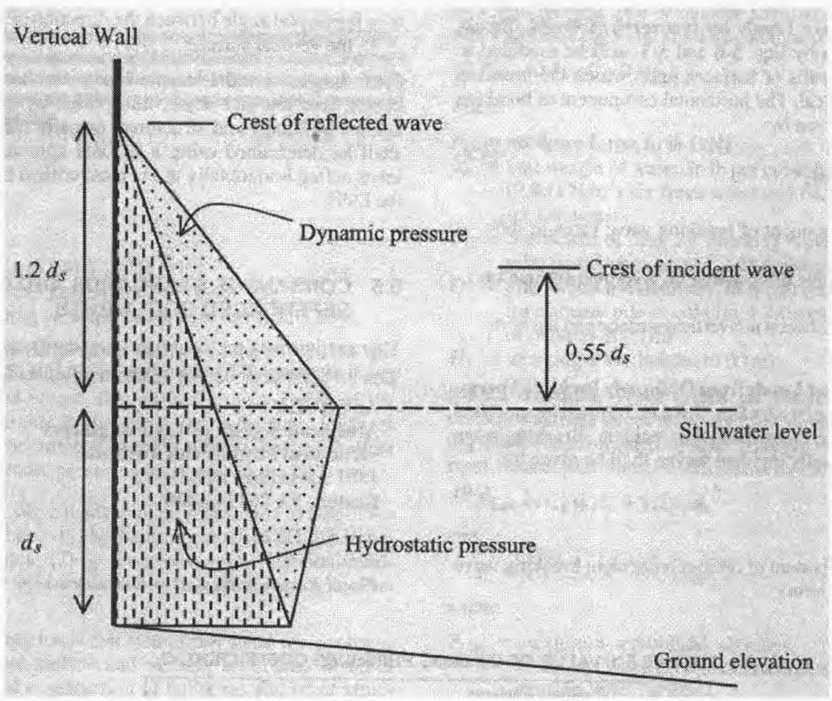

Figure 4. Wave pressures of normally incident wave breaking on a vertical wall, source: (ASCE/SEI 7-05, 2006).

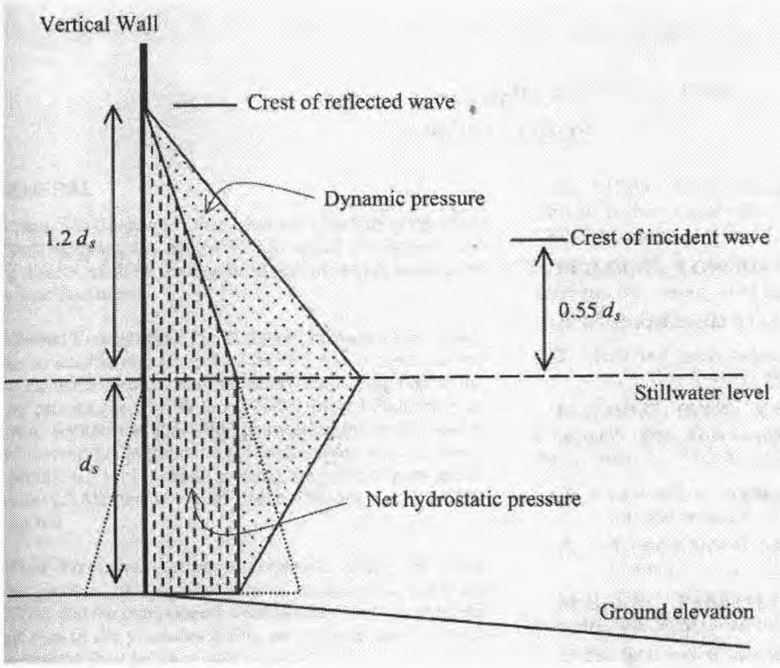

Figure 5. Normally incident breaking wave pressures acting on a vertical wall, source: (ASCE/SEI 7-05, 2006).

FEMA – Coastal Construction Manual – 2000

The Coastal Construction Manual of the Federal Emergency Management Agency provides a set of guidelines primarily intended for building type constructions located on coastal areas (FEMA, 2000). Chapter 11 of the Coastal Construction Manual describes flood and wave loads.

Design flood

For communities that adhere to the National Flood Insurance Program (NFIP), the design flood is equal to the base flood, the flood that has a 1% probability of being equaled or exceeded in any given year. The design flood should always be greater than or equal to the base flood.

Design flood elevation

This document defines a Design Flood Elevation (DFE), which can be higher than the Base Flood Elevation (BFE) if the local officials choose a freeboard. The DFE should be equal or higher that the BFE. Figure 6 shows a schematic of the design flood elevations and other flood parameters.

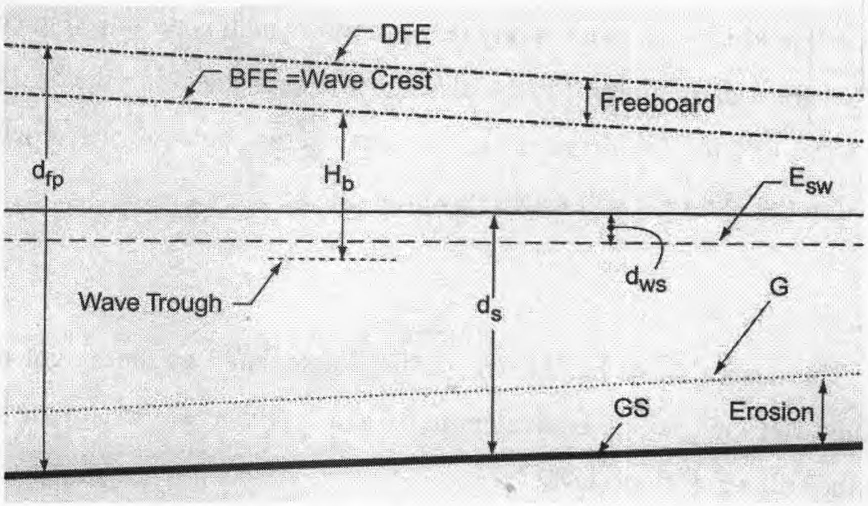

Figure 6. Parameters that determine flood depth, source: (FEMA, 2000).

The labels in Figure 6 represent the following parameters: *DFE* = Design Flood Elevation in feet above datum, d_{fp} = design flood protection in feet, *BFE* = Base Flood Elevation in feet above datum, *freeboard* = vertical distance in feet between *BFE* and *DFE*, H_b = breaking wave height = 0.78 d_s (note that 70% of wave height lies above E_{sw}), E_{sw} = design still water flood elevation in feet above datum, d_{ws} = wave setup in feet, d_s = design still water flood depth in feet, *G* = ground elevation, existing or pre-flood, in feet above datum, *Erosion* = loss of soil during design flood event in feet (not including effects of localized scour), *GS* = lowest eroded ground elevation adjacent to building in feet above datum (including the effects of localized scour).

Design flood depth

The design flood depth is given by the following equation:

$$d_s = E_{sw} + d_{ws} - GS \qquad \text{Equation 11}$$

where all the terms are as defined before.

Wave setup

FEMA recommends checking for wave setup, d_{ws}, in the *Hydrologic Analyses* section of the Flood Insurance Study (FIS) report, which is produced in conjunction with the FIRM for a community. FEMA also recommends checking the *Stillwater Elevation* table of the FIS for footnotes related to wave setup, because wave setup may not be included in the 100-year still water elevation.

Design wave height

The design wave height, H_b, shall be calculated as the height of depth-limited breaking waves, which are equivalent to 0.78 d_s. In this case 70% of the wave height lies above the still water flood level.

Design flood velocity

FEMA states that the estimation of design flood velocity in coastal flood hazard areas is highly uncertain. FEMA recommends flood velocities to be estimated conservatively, that is, assuming floodwaters can approach the structure from the most critical direction with a high velocity. FEMA provides the flowing equations to estimate flood velocity:

Lower bound $\quad V = d_s/t \quad$ Equation 12

Upper bound $\quad V = \sqrt{gd_s} \quad$ Equation 13

Extreme (tsunami) $\quad V = 2\sqrt{gd_s} \quad$ Equation 14

where,

V = design flood velocity, *ft/sec*

d_s = design still water flood depth, *ft*

t = 1 *sec*

g = gravitational constant (32.2 ft/sec^2)

FEMA recommends the design flood velocity in coastal areas to be taken between the upper and lower bounds. It is recommended that the lower bound be used for constructions located near the flood source or other buildings that may confine flood waters and increase flood velocities. It is advised to use the lower bound velocity where the structure is located in a site with a gentle slope and is unaffected by other structures. An equation is also given to estimate flood velocity for extreme events such as a tsunami.

Hydrostatic loads

FEMA also describes hydrostatic loads, and the hydrostatic force per unit width is taken as:

$$f_{sta} = \frac{1}{2}\gamma d_s^2 \qquad \text{Equation 15}$$

where,

f_{sta} = hydrostatic force per unit width (*lb/ft*) resulting from loading against a vertical element with no water on the other side

γ = specific weight of water (62.4 lb/ft^3 for fresh water and 64.0 lb/ft^3 for salt water)

d_s = design still water flood depth in feet

Buoyancy force

$$F_{buoy} = \gamma Vol \qquad \text{Equation 16}$$

where γ is as described before and,

F_{buoy} = vertical hydrostatic force in *lb* resulting from the displacement of a given volume of flood water

Vol = volume of flood water displaced by a submerged object in ft^3

Wave loads

Wave load calculation requires knowledge of wave heights, which are assumed to be depth limited at the site of interest in the FEMA manual. FEMA uses its Wave Height Analysis for Flood Insurance Studies (WHAFIS) to estimate wave heights and wave crest elevations and recommends designers to use the results of that analysis to calculate wave loads directly.

Wave forces are divided into four categories:

1. Forces from non-breaking waves - can be computed as hydrostatic forces acting against piles.
2. Forces from breaking waves - will be of short duration but high magnitude.
3. Forces from broken waves - are similar to hydrodynamic forces caused by flowing of surging water.
4. Forces from uplift - usually caused by wave runup, deflection, or peaking against the underside of horizontal surfaces.

The manual recommends the breaking wave load to be used as the design wave load, since it is considered the most severe. Breaking wave loads are divided into those breaking on small diameter vertical elements and those breaking on walls.

Breaking wave loads on vertical piles

The breaking load on a pile is computed with the following equation and is assumed to act at the still water level:

$$F_{brkp} = \frac{1}{2} C_{db} \gamma D H_b^2 \qquad \text{Equation 17}$$

where,

F_{brkp} = Drag force acting at the still water level, *lb*

C_{db} = Breaking wave drag coefficient (2.25 for square or rectangular piles and 1.75 for round piles)

D = Pile diameter, *ft*

H_b = Breaking wave height in feet (0.78 d_s)

γ = Specific weight of water (62.4 lb/ft^3 for fresh water and 64 lb/ft^3 for salt water)

d_s = Design still water flood depth, *ft*

Breaking wave loads on vertical walls

The design of walls assumes the vertical wall causes a standing wave to form on the seaward side of the wall and that the crest of the wave reaches a height of 1.2 d_s above the still water elevation. The breaking wave load per unit length of wall is given by the following equations.

Case 1. Enclosed dry space behind wall

$$f_{brkw} = 1.1 C_p \gamma d_s^2 + 2.41 \gamma d_s^2 \qquad \text{Equation 18}$$

Case 2. Equal still water level on both sides of wall

$$f_{brkw} = 1.1 C_p \gamma d_s^2 + 1.91 \gamma d_s^2 \qquad \text{Equation 19}$$

where,

f_{brkw} = Total breaking wave load per unit length of wall (*lb/ft*) acting at the still water level

C_p = Dynamic pressure coefficient from Table 1

γ = Specific weight of water (62.4 lb/ft^3 for fresh water and 64 lb/ft^3 for salt water)

d_s = Design still water flood depth in feet

Table 1. Value of dynamic pressure coefficient as a function of probability of exceedance (FEMA, 2000)

Cp	Building type	Probability of exceedance
1.6	Accessory structure, low hazard to human life or property in the event of failure	0.5
2.8	Coastal residential building	0.01
3.2	High-ocupancy building or critical facility	0.001

The resulting static and dynamic pressures are shown on Figure 7.

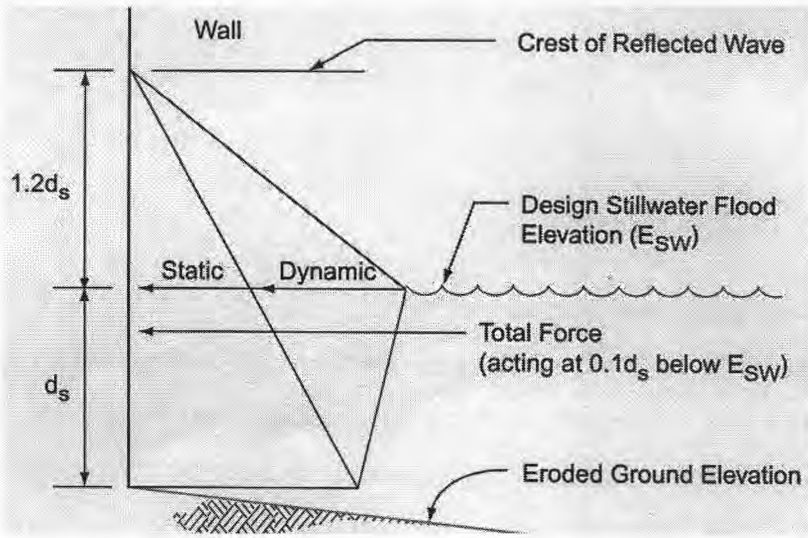

Figure 7. Static and dynamic wave pressure distribution on a vertical wall, source: (FEMA, 2000).

Hydrodynamic loads

The FEMA manual assumes hydrodynamic loads imposed by water velocities lower than 10 ft/sec can be converted to an equivalent hydrostatic load using the following expressions:

$$d_{dyn} = \frac{1}{2} C_d \frac{V^2}{g} \qquad \text{Equation 20}$$

where,

d_{dyn} = Equivalent additional flood depth to be applied to the upstream side of the affected structure, *ft*

V = Velocity of water in ft/sec from Equations 12 through 14

g = Acceleration due to gravity (32.2 *ft/sec*^{2})

C_d = Drag coefficient (2.0 for square or rectangular piles, 1.2 for round piles or from Table 2 for large obstructions)

$$f_{dyn} = \gamma d_s d_{dyn} \qquad \text{Equation 21}$$

where,

f_{dyn} = Equivalent hydrostatic force per unit width (*lb/ft*) due to low-velocity flow acting at the point 2/3 below the still water surface

γ = Specific weight of water (62.4 lb/ft^3 for fresh water and 64 lb/ft^3 for salt water)

The manual recommended the drag coefficient be estimated using Figure 8 and considering: (a) the ratio of the width of the element, *w*, to the height of the element, *h*, for fully immersed elements, or (b) the ratio of the width of the element, *w*, to the still water depth, d_s if the element is not fully immersed in water. The recommended drag coefficients are indicated in Table 2.

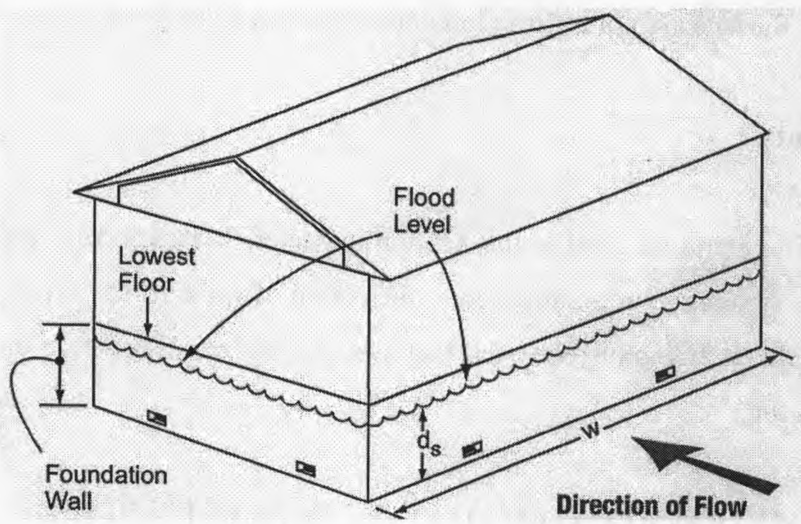

Figure 8. Determination of drag coefficient, source: (FEMA, 2000).

Table 2. Drag coefficients for ratios of w/d_s or w/h

Width to depth ratio (w/d_s or w/h)	Drag coefficient C_d
From 1-12	1.25
13-20	1.3
21-32	1.4
33-40	1.5
41-80	1.75
81-120	1.8
>120	2.0

For water velocities greater than 10 ft/sec the following expression can be used to obtain the horizontal drag force:

$$F_{dyn} = \frac{1}{2} C_d \rho V^2 A \qquad \text{Equation 22}$$

where,

F_{dyn} = Horizontal drag force in lb acting at the still water mid-depth

Cd = Drag coefficient (2.0 for square or rectangular piles, and from Table 2 for larger obstructions)

ρ = Mass density of fluid (1.94 *slugs/ft*^{3} for fresh water and 1.99 *slugs/ft*^{3} for salt water)

V = Velocity of water in *ft/sec* from Equations 12 through 14

A = Surface area of obstruction normal to flow in $ft^2 = wd_s$ or hw, see Figure 8

Comments

The literature cited in this section indicates that a specific method for the design of bridge superstructures subjected to the action of wave forces is not provided in any of the guidelines. It can also be seen that some available information on this topic is even contradictory.

INFORMATION RELATED TO WAVE FORCES ON BRIDGE SUPERSTRUCTURE

This section includes summaries of research papers, book chapters, and research reports that contain information related to wave forces on elements similar to bridge decks.

Tedesco et al. – Response of structures to water waves – 1999

This section shows a summary of a section of the book Structural Dynamics by Tedesco et al. (Tedesco et al., 1999). The authors indicated that pressure and drag produce the main hydrodynamic forces acting on structures. The interaction between a structure and waves is greatly influenced by the size of the structure relative to the wavelength, L. The following observations hold for a structure such as pile characterized by its diameter, D. If D/L is small then the Morison equation can be used to estimate forces, since wave diffraction is negligible. If D/L is large, diffraction theory is used to estimate forces, since the structure modifies the wave field significantly. When the wave field is not greatly modified by the structure and the drag forces are small, the forces are dominated by inertia and can be estimated by the Froude-Krylov method (Tedesco et al., 1999).

A wave field is said to not be affected by the presence of a structure when the ocean waves just a wavelength away from the structure (50 to 100 pile diameters in the case of the pile) the waves seem to be unaffected by the presence of the structure.

The wave field may be significantly affected by the presence of a structure such as in the case of a floating dock, where some wave energy travels around and under the dock, while an important portion of the incident wave is reflected.

Morison equation

If the diameter of the structure is less than 5% of the wave length the assumption that the wave field is not affected by the structure is reasonable. Some examples of these types of structures include structural elements in oil platforms, piles, pipelines, and moorings. The Morison equation is the most common tool used to estimate the in-line wave force on small bodies.

Consider a horizontal pressure component induced by the wave on a vertical cylinder as indicated in Figure 9. Applying Bernoulli's equation, the fluid pressure is given by:

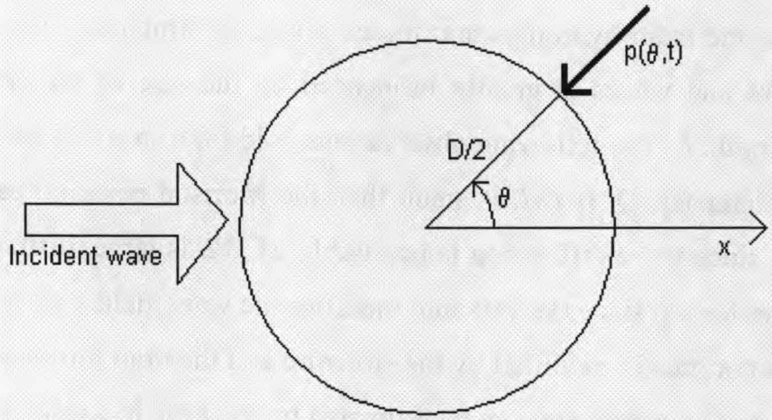

Figure 9. Pressure induced by wave flow through a cylinder (Tedesco et al., 1999).

$$p = -\rho\frac{\partial\phi}{\partial t} - \frac{\rho}{2}\left(u_r^2 + u_\theta^2\right) - \rho g z + C_B \qquad \text{Equation 23}$$

Where ρ and θ are the polar coordinates, u is the water particle velocity, ϕ is the velocity potential, and C_B is the Bernoulli constant. Integrating the pressure over the circumference gives the following force per unit length of cylinder in the wave direction:

$$f_{ix} = -\int_{-\pi}^{\pi} p\left(\frac{D}{2},\theta,t\right)\cos\theta\frac{D}{2}d\theta \qquad \text{Equation 24}$$

Thus the horizontal force per unit length of cylinder is:

$$f_{ix} = \left(1 + C_a\right)\rho\frac{\pi D^2}{4}\frac{du}{dt} \qquad \text{Equation 25}$$

This force is called the inertia force because it is proportional to the acceleration of the fluid. The coefficient C_a is called the added mass coefficient and is equal to one for a vertical circular cylinder. An inertia coefficient that accounts for different geometries is given by:

$$C_m = 1 + C_a \qquad \text{Equation 26}$$

where C_m is called the inertia coefficient.

In addition to the inertia forces, drag forces will develop on the structure due to fluid-structure interaction. A drag force will develop from friction between the fluid and the structure, and another force results from a differential of pressure across the structure when the flow separates. The total drag force from the two sources can be written as:

$$f_{dx} = \frac{1}{2}\rho C_d D|u|u \qquad \text{Equation 27}$$

where,

f_{dx} = Drag force per unit length of a cylinder in the direction of flow (x in this case)

C_d = Drag force coefficient

u = Water particle velocities, *ft/sec*

Assuming the drag and inertia forces can be added, the Morison equation is obtained:

$$f_x = f_{dx} + f_{ix} = \frac{1}{2}\rho C_d D|u|u + \rho C_m \frac{\pi D^2}{4}\frac{du}{dt} \qquad \text{Equation 28}$$

In Equation 28 it is assumed the pile is not present when calculating the water particle velocity and acceleration at the center of the pile.

If linear wave theory is used to compute fluid velocity and acceleration at x = 0 (the center of the pile), the Morison equation becomes:

$$f_x = C_d f_{xd} + C_m f_{xm} \qquad \text{Equation 29}$$

where,

$$f_{xd} = \frac{1}{8}\rho D H^2 \omega^2 \frac{\cosh^2[k(h+z)]}{\sinh^2(kh)}|\cos(-\omega t)|\cos(-\omega t) \qquad \text{Equation 30}$$

$$f_{xm} = \frac{\pi}{8}\rho D^2 H \omega^2 \frac{\cosh[k(h+z)]}{\sinh^2(kh)}\sin(-\omega t) \qquad \text{Equation 31}$$

The Keulegan-Carpenter number affects the magnitude of the drag and inertia coefficients shown in previous equations.

$$K = \frac{u_m T}{D} \qquad \text{Equation 32}$$

where K is the Keulegan-Carpenter number, u_m is the magnitude of the horizontal velocity, T is the wave period, and D is the diameter of the structure.

Force coefficients

Inaccurate predictions can be made when using linear wave theory to determine the drag and inertia coefficients. This happens because linear wave theory cannot make predictions for force values above the still water level (SWL), while the largest forces develop near the wave crest in reality. It is common engineering practice to use advanced nonlinear theories such as Stokes 5^{th} or stream function theory.

Marine plants and animals often develop on structural elements. This growth does not contribute to structural stiffness, however, it does increase the weight of structural elements. These biofouling also increase the drag and inertia coefficients, as well as the diameter of the structural elements. Examples of these plants and animals range from soft, such as sponges and seaweed, to hard, such as barnacles and mussels. Table 3 illustrates drag and inertia coefficients for typical structural shapes without including any biofouling effects. It should be mentioned that the drag and inertia coefficients depend on the Reynolds number and the Keulegan-Carpenter number (Sarpkaya, 1981; Wilson, 2003). For a dependence on the drag coefficient on the Reynolds number, see Figure 10 (Çengel and Cimbala, 2006).

Table 3. Drag and inertia coefficients for typical geometries, source: (Tedesco et al., 1999).

Section Shape	C_d	C_m
→ □	2.0	2.5
→ ▢	0.6	2.5
→ ▷	2.0	2.3
→ ◁	1.3	2.3
→ ◇	1.5	2.2

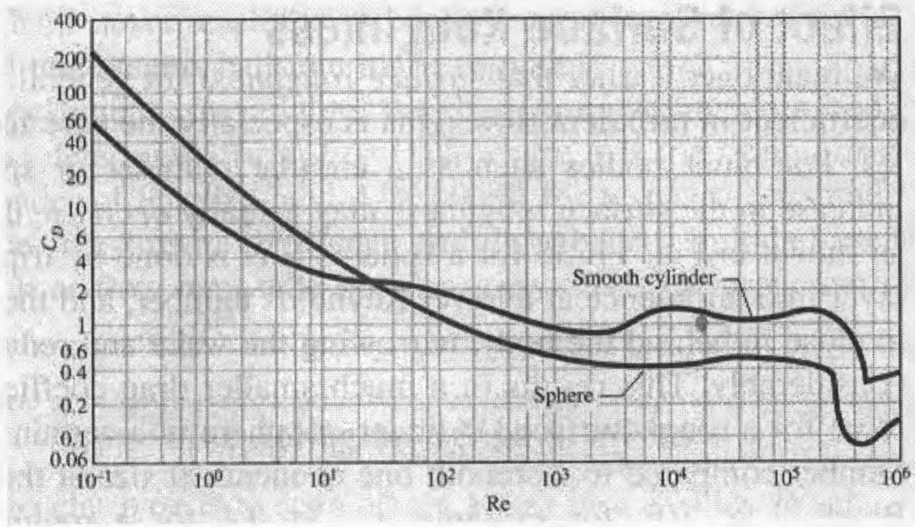

Figure 10. Average drag coefficient for cross flow over a smooth cylinder and a smooth sphere, source: (Cengel and Cimbala, 2006).

Lwin – Floating bridges – 1999

Floating bridges are superstructures typically subjected to sea currents and sea waves. Therefore, as an introduction to the parameters required for the design of bridges exposed to water forces induced by hurricanes, a description of the design factors that are commonly applied to floating bridges will be given in this section.

A large number of bridges span waterways. However, to span large bodies of water with considerable depths and soft sea bottom, conventional piers are impractical, and floating bridges can be cost-effective solutions (Lwin, 1999). Floating bridges have been built for centuries for military operations. Modern floating bridges can be made of concrete, wood, steel, or a combination of materials.

The design of floating bridges needs to conform to AASHTO Bridge Design Specifications as much as possible (Lwin, 1999). The performance of a floating bridge is highly sensitive to environmental forces such as those imposed by waves, winds, and currents.

Winds and waves are the major environmental loads. The environmental loads induce horizontal, vertical, and torsional loads on a floating bridge (Lwin, 1999). These loads are a function of wind speed, wind direction, wind duration, fetch length, channel configuration, and depth. Floating bridges are typically designed for normal storm conditions, which is the maximum storm that is likely to occur once a year. Floating bridges are also designed for extreme conditions, which are caused by the maximum storm likely to occur once in 100 years (Lwin, 1999). Lwin provides some recommendations for load factors to be used in the design of floating bridges following the AASHTO Bridge Design Specifications (Lwin, 1999).

Floating bridges are typically built using a box girder structure, with segments to control progressive failure (Lwin, 1999; Leira and Langen, 1984).

The design of floating bridges may require a dynamic analysis. Leira and Langen used a probabilistic dynamic analysis method to study a floating bridge using finite elements (Leira and Langen, 1984). In this paper the authors modeled the sea waves with a harmonic function.

Shih and Anastasiou – Wave induced uplift pressures acting on a horizontal platform – 1989

A report by Shih and Anastasiou looks at experimental values of wave loads on horizontal platforms (Shih and Anastasiou, 1989). The experimental data is validated through the hindcasting of wave data obtained in Maya Quay, Kobe, during a typhoon in 1964. The authors used their measurements and the best-fit technique to modify Teruaki Furudoi's formula for uplift force:

$$\frac{F_{mean}}{\rho g w H_c c} = 10.91 * \left(\frac{H_u}{d_o}\right) - 10.91 \qquad \text{Equation 33}$$

where,

F_{mean} = Mean impact force

ρ = Specific water density

w = Width of the platform

H_c = Wave crest height above mean water level

c = Clearance of the platform above mean water level

and

$$H_u = H_o\left\{1 + \left(\pi H_o / L_o\right)\coth\left(2\pi h_o / L_o\right)\right\} \qquad \text{Equation 34}$$

where,

H_o = Height of incident waves at the off-sea

L_o = Deep water wave length

h_o = Water depth

d_o = Distance between the still water surface and the apron

Equation 34 yielded results compatible with those hindcasted at the site. These being F_{mean} = 5.2 ton/m and F_{max} = 8.0 ton/m. Note when solving for F_{max} to replace F_{mean} with F_{max} and replace 10.91 with 16.67.

The authors also examined three different types of pressure: slow varying positive pressure, P_{+ve}, slow varying negative pressure, P_{-ve}, and impact pressure, P, for different clearance and wave types. These experiments produced maximum values of 1.52 KN, 0.72 KN, and 19.48 KN/m² for P_{+ve}, P_{-ve}, and P, respectively. The authors concluded the slowly varying positive pressure has two components: the hydrostatic head due to the wave crest elevation, and the hydrodynamic head caused by the wave induced fluid motion; although when the platform is free from any lateral constraints, the P_{+ve} is less than the hydrostatic head alone. The slowly varying negative pressure is independent of clearance, but depends greatly on the width of the platform. While the impact pressure, P, is dependent on the wave height, platform clearance, and the properties of the wave impacting the structure.

Suchithra and Koola – A study of wave impact on horizontal slabs – 1995

A paper written by Suchithra and Koola examines the use of stiffeners in deck design and the variation in the slamming coefficient C_s, which is used to find the vertical forces imposed by slamming waves. The vertical force is found using:

$$F_s = \frac{1}{2} C_s \rho A V^2 \qquad \text{Equation 35}$$

where,

F_s = Slamming force

A = Area of contact

ρ = Mass density of water

V = Vertical water particle velocity

C_s = Slamming coefficient

Equation 35 can only be effectively used if a valid value of C_s is known. The authors obtained experimental values for C_s ranging from 2.5 to 10.2, but also found the coefficient to be dependent on the wave frequency. The authors then defined a modified slamming coefficient, C_{ns}, to be used for design purposes independent of frequency. This modified slamming coefficient may be found using:

$$C_{ns} = C_s \, d/L \qquad \text{Equation 36}$$

where,

d = Deck clearance

L = Deep water wave length

A mean value of 1.7 was obtained for C_{ns}, which could be used in design due to its frequency independence (Suchithra and Koola, 1995).

Bea et al. – Wave forces on decks of offshore platforms – 1999

Isaacson and Prasad stated that the total forces imposed on an offshore platform deck could be formulated as (Isaacson and Prasad, 1992):

$$F_{tw} = F_b + F_s + F_d + F_l + F_i \qquad \text{Equation 37}$$

where,

F_b = Buoyancy force (vertical)

F_s = Slamming force

F_d = Drag (velocity-dependent) force

F_l = Lift (velocity-dependent, normal to wave direction) force

F_i = Inertia (acceleration dependent)

The force idealized by Isaacson and Prasad is shown in Figure 11.

Slamming force

A horizontal slamming force can be estimated with the expression (Bea et al., 1999):

$$F_s = 0.5 C_s \rho A u^2 \qquad \text{Equation 38}$$

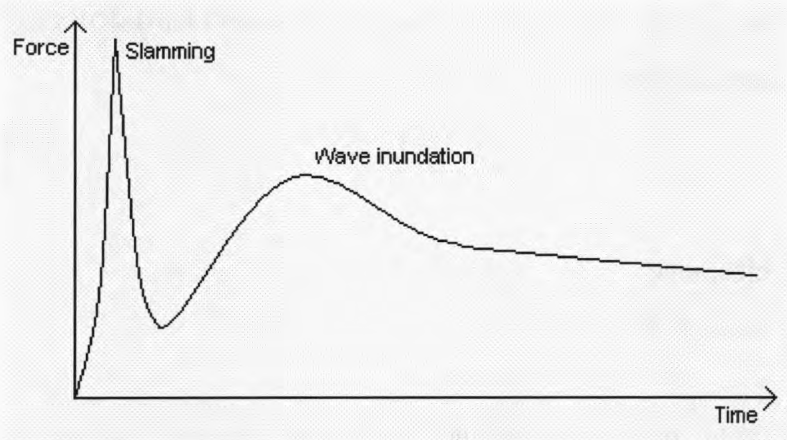

Figure 11. Idealized wave force on a platform deck.

where,

F_s = Slamming force

C_s = Slamming coefficient

ρ = Mass density of seawater (= 1.99 $slugs/ft^3$ for seawater)

A = Vertical deck area subjected to the wave crest

u = Horizontal fluid velocity in the wave crest

Isaacson and Prasad asserted that C_s could vary approximately between π and 2π.

According to Bea et al., the effective slamming force can be obtained by including a dynamic load factor:

$$F_{se} = F_e F_s \qquad \text{Equation 39}$$

where,

F_{se} = Effective slamming force

F_e = Dynamic load factor

F_s = Slamming force

The value of the dynamic load factor depends on the relative values of the duration of loading and the period of vibration of the structure. Bea et al. indicate that the dynamic load factor is equal to:

$$DAF = 2\pi\alpha\left(t_d / T_n\right) \qquad \text{Equation 40}$$

where,

t_d = duration of the impact loading

T_n = natural period of the deck

α = reflects the time-magnitude characteristics of the impact loading ($\alpha = 0.5$ for triangular loading and $\alpha = 2/\pi$ for half-sine loading).

Inundation forces

The horizontal drag force can be estimated with the equation:

$$F_d = 0.5\rho C_d A u_h^2 \qquad \text{Equation 41}$$

where,

F_d = Horizontal drag force

C_d = Drag coefficient

A = Horizontal area

u_h = Horizontal velocity of water particles

The vertical lift force can be found with the expression:

$$F_l = 0.5\rho C_l A u_v^2 \qquad \text{Equation 42}$$

where,

F_l = Vertical lift force

C_l = Lift coefficient

A = Vertical area

u_v = Vertical velocity of water particles

The horizontal inertial force can be determined as:

$$F_i = \rho C_m V a \qquad \text{Equation 43}$$

where,

F_i = Inertial force

C_m = Inertia coefficient

V = Volume of deck inundated

a = Horizontal acceleration of water particles

McConnell et al. – Piers, jetties, and related structures exposed to waves – 2004

A research report by McConnell et al. presents a methodology to estimate wave forces on horizontal elements (McConnell et al., 2004). The authors adopt the Rayleigh distribution as a first approximation to the distribution of individual wave heights. With this assumption, the most probable value of the maximum wave height H_{max} can be estimated with the relationship:

$$\left[\frac{H_{\max}}{H_{1/3}}\right]_{\mathrm{mode}} \approx 0.706\sqrt{\ln N_z} \qquad \text{Equation 44}$$

where,

H_{max} = Maximum wave height

$H_{1/3}$ = Significant wave height

N_z = Number of waves (can be calculated knowing the wave period and assuming a storm duration)

The authors follow Stansber's approximation to estimate the crest height in deep water as:

$$\eta_{\max} = \frac{H_{\max}}{2}\exp\left(\frac{2\pi}{L_m}\frac{H_{\max}}{2}\right) \qquad \text{Equation 45}$$

where,

η_{max} = expected maximum crest elevation, *ft*

L_m = Wave length, *ft*

H_{max} = Maximum wave height, *ft*

McConnell et al. report the results of a series of experiments made on a model of a platform deck. The model was designed to resemble the configuration and dimensions of a typical platform. The model was made to a scale of 1:50 of a typical offshore structure. The waves used to test the specimen were also representative of an offshore structure.

The model was tested with three configurations: (a) deck with beams, (b) flat deck (no beams), and (c) deck with beams and side panels. The parameters used in the test modelled the following conditions: H_s = 2.5 to 5.5 m, T_m = 5 to 15 s, water depth 18.75 and 15 m, clearance 0.25 to 4 m, relative water depth (h/L_m) = 0.48, and sampling frequency 40 Hz.

The authors recorded the three force parameters defined next and shown in Figure 12.

F_{max} = Impact force

$F_{qs+,\, v\ or\ h}$ = Maximum positive (upward or landward) quasi-static force

$F_{qs-,\, v\ or\ h}$ = Maximum negative (downward or seaward) quasi-static force

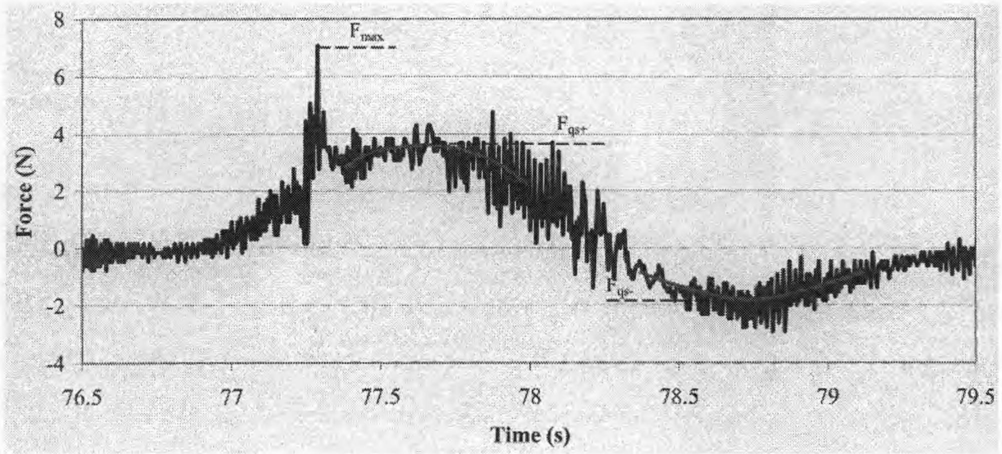

Figure 12. Force parameters, source: (McConnell et al., 2004).

The authors modelled the design wave with a maximum crest elevation as shown in Figure 13. According to this diagram, the hydrostatic pressures acting on the side and bottom of a deck are:

$$p_1 = (\eta_{\max} - b_h - c_1)\rho g \qquad \text{Equation 46}$$

$$p_2 = (\eta_{\max} - c_1)\rho g \qquad \text{Equation 47}$$

where,

p_1 = Pressure at the top of the deck

p_2 = Pressure at the bottom of the deck

b_w = Deck width

b_h = Deck height

b_l = Deck length

c_1 = Clearance

η_{max} = Maximum wave crest elevation

Thus, the hydrostatic horizontal wave force is:

$$F_h^* = b_w(\eta_{max} - c_1)\frac{p_2}{2} \qquad \text{for } \eta_{max} \leq c_1 + b_h \qquad \text{Equation 48}$$

$$F_h^* = b_w b_h \frac{p_1 + p_2}{2} \qquad \text{for } \eta_{max} \rangle c_1 + b_h \qquad \text{Equation 49}$$

and the hydrostatic vertical wave force is:

$$F_v^* = b_w b_l p_2 \qquad \text{Equation 50}$$

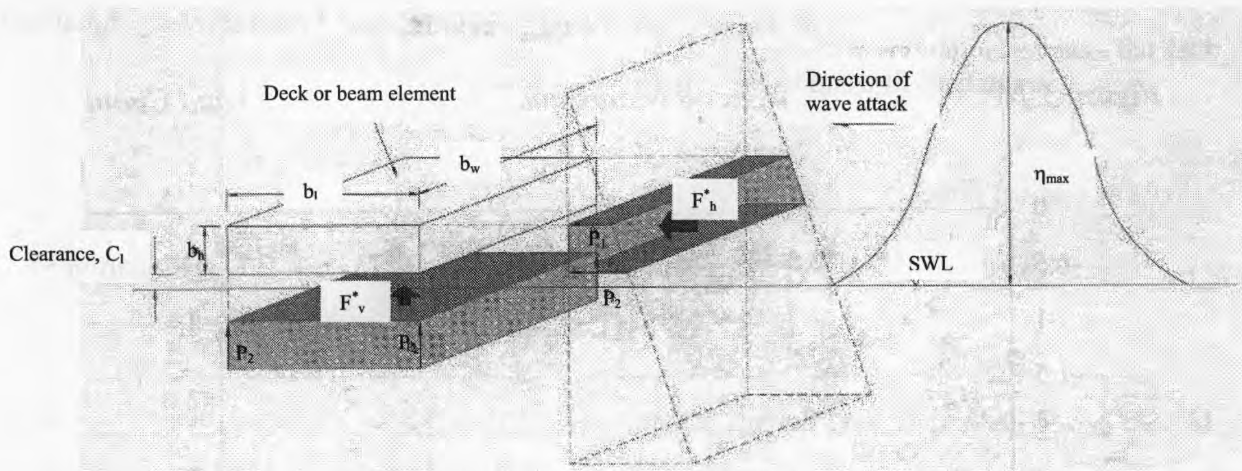

Figure 13. Definition of wave forces, modified from: (McConnell et al., 2004).

According to the experimental studies carried out by the authors, the ratio of the measured wave forces (F_{qs+} or F_{qs-} as defined in Figure 12) to the hydrostatic forces (F_h^* or F_v^*) for different ratios of maximum freeboard (η_{max}-c_1) to significant wave height are given in a set of plots. The forces described are the average of the highest four values recorded in 1000 waves ($F_{1/250}$). For the case of upward forces on beams and decks (ratio of F_{qs+} to F_v^*) the maximum-observed ratio of wave load to hydrostatic force is 4.5. For downward forces (ratio of F_{qs-} to F_v^*) the maximum-recorded ratio is 2.3. The maximum ratio for horizontal forces (ratio of F_{hqs} to F_h^*) is approximately 11.

The authors also measured impact wave forces on the model. The maximum values recorded were as follows: the ratio of the maximum observed vertical impact force over the quasi-static wave force (ratio of F_{max} to F_{vqs+}) was approximately 5, following the definitions of Figure 12. As far as the horizontal force is concerned, the maximum observed impact ratio (ratio of F_{max} to F_{hqs+}) was approximately 7.

The authors indicate that according to laboratory studies vertical loads can be higher than horizontal loads.

From the results of their experiments the authors found the following equations based on the best-fit trend to the experimental data.

For vertical forces:

$$\frac{F_{vqs(+or-)}}{F_v^*} = \frac{a}{\left[\dfrac{\eta_{\max} - c_l}{H_s}\right]^b} \qquad \text{Equation 51}$$

The best-fit coefficients for upward vertical forces (seaward beam and deck) were $a = 0.82$ and $b = 0.61$, and for downward vertical forces (seaward beam and deck) the coefficients were $a = -0.54$, $b = 0.91$.

For horizontal forces:

$$\frac{F_{hqs(+or-)}}{F_h^*} = \frac{a}{\left[\dfrac{\eta_{\max} - c_l}{H_s}\right]^b} \qquad \text{Equation 52}$$

The best-fit coefficients for the case of shoreward horizontal forces (seaward beam) were $a = 0.45$ and $b = 1.56$, while for seaward horizontal forces (seaward beam) were $a = -0.20$ and $b = 1.09$.

Goda – Random seas and design of maritime structures – 2000

Goda presents an overview of the development of wave pressure formulas (Goda, 2000). The formula proposed by Hiroi in 1919 yields a pressure as a function of wave height:

$$p = 1.5\rho g H \qquad \text{Equation 53}$$

where,

p = Pressure assumed to act uniformly over the full height of an upright section, or to an elevation of 1.25 times the wave height above the still water level, whichever is less

ρ = Density of seawater

g = Acceleration of gravity

H = Incident wave height

Where wave information was scarce, Hiroi recommended using a design wave height of 0.9 times the water depth. During the development of design equations engineers debated whether to use $H_{1/3}$, $H_{1/10}$, or H_{max} as the design wave, concluding that H_{max} should be substituted in the wave pressure formulas.

The wave pressure distribution proposed by Goda is illustrated in Figure 14. This figure helps clarify the meaning of the terms involved in the pressure coefficients proposed by the author. The equation is applicable to breaking and non-breaking waves. The terms shown in the figure denote the following: h, water depth in front of the breakwater, d, depth above the armor layer of the rubble foundation, h', distance from the design water level to the bottom of the upright section, and h_c, crest elevation of the breakwater above the design water level.

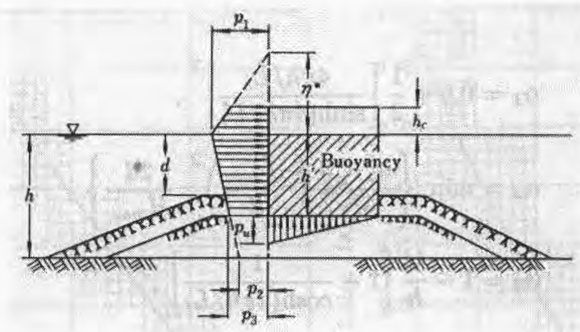

Figure 14. Wave pressure distribution on the vertical section of a breakwater, source: (Goda, 2000).

Goda specifies that the highest wave in the design sea state should be used. Its height should be taken as H_{max} = 1.8 $H_{1/3}$ seaward of the surf zone, whereas within the surf zone the height should be taken as the highest random breaking wave H_{max} at the location at a distance $5H_{1/3}$ seaward of the breakwater. $H_{1/3}$ should be estimated at the depth of the location of the breakwater. The period of the highest wave is taken as that of the significant wave: $T_{max} = T_{1/3}$.

Goda specifies that the elevation to which the wave pressure is exerted be:

$$\eta^* = 0.75(1 + \cos\beta)H_{\max} \qquad \text{Equation 54}$$

where,

β = Angle between the direction of wave approach and a line normal to the breakwater. Due to the uncertainty of the wave direction, the principal wave direction should be rotated 15° toward the line normal to the breakwater.

The wave pressure on the front of a vertical wall is thus:

$$p_1 = \frac{1}{2}(1 + \cos\beta)(\alpha_1 + \alpha_2 \cos^2\beta)\rho g H_{\max} \qquad \text{Equation 55}$$

$$p_2 = \frac{p_1}{\cosh(2\pi h/L)} \qquad \text{Equation 56}$$

$$p_3 = \alpha_3 p_1 \qquad \text{Equation 57}$$

where,

$$\alpha_1 = 0.6 + \frac{1}{2}\left[\frac{4\pi h/L}{\sinh(4\pi h/L)}\right]^2 \quad \text{Equation 58}$$

$$\alpha_2 = \min\left\{\frac{h_b - d}{3h_b}\left(\frac{H_{\max}}{d}\right)^2, \frac{2d}{H_{\max}}\right\} \quad \text{Equation 59}$$

$$\alpha_3 = 1 - \frac{h'}{h}\left[1 - \frac{1}{\cosh(2\pi h/L)}\right]^2 \quad \text{Equation 60}$$

h_b = water depth at the location at a distance $5H_{1/3}$ seaward of the breakwater

L = Wave length at the structure

The previous equations are assumed to hold even in the case of wave overtopping.

The buoyancy pressure is calculated for the displaced volume of the structure in still water below the design water level. The uplift pressure acting at the bottom of the structure is assumed to have a triangular distribution with toe pressure equal to:

$$p_u = \frac{1}{2}(1 + \cos\beta)\alpha_1\alpha_3\rho g H_{\max} \quad \text{Equation 61}$$

H_{max} is used in the previous equation based on the philosophy that a breakwater should be designed to be safe against a wave with the largest pressure among storm waves. Goda recommends a value of H_{max} = 1.8 $H_{1/3}$ based on performance of many prototype breakwaters. However, the design engineer could select H_{max} to have a different value. The criterion used in deriving the equation proposed by Goda recognizes that the greatest wave pressure is exerted not by waves just breaking at the site, but by waves which have already begun to break at a short distance seaward of the breakwater, midway through the plunging distance. The value of the empirical coefficient α_1 in the pressure intensity p_1 has been determined based on tendency for wave pressure to increase with the wave period. The equation for coefficient α_2 represents the tendency of the pressure to increase with the rubble foundation height. Coefficient α_3 was derived assuming a linear pressure variation between p_1 and p_2 along a vertical wall.

Goda also mentioned that the wave pressure exerted on the upright section of a vertical breakwater is approximately proportional to the height of the wave incident on the breakwater, and is to some extent influenced by the wave period, the seafloor slope, and the shape and dimensions of the rubble mound foundation among other factors. Laboratory tests indicated that the breaking wave pressure increases as the seafloor slope becomes steeper. The wave pressure and the width of the upright section of the breakwater decrease gradually as the incident wave angle decreases.

Goda also addressed the topic of impulsive wave pressure. He states that the impulsive pressure has a very short duration, although it may rise to over an order of magnitude above the hydrostatic pressure corresponding to the wave height. The author states that with an increase in the incident angle of the wave, the impulsive pressure decreases rapidly. A questionnaire based mostly on the work of Mitsuyasu is shown in Figure 15 to evaluate the danger of impulsive breaking wave pressure (Mitsuyasu, 1962). The angle between a line the normal to the breakwater longitudinal axis and the line normal to the wave longitudinal axis is called the angle of incidence. Goda explains that a Japanese document written by Tanimoto suggested that if the angle of incidence is greater than 20°, the danger of impulsive breaking wave pressure is small (Tanimoto, 1976).

the design of structural parts against slamming loads (Hagiwara and Yuhara, 1976). Hagiwara and Yuhara found that by introducing an equivalent static pressure in analyzing the strain of a rectangular panel due to slamming load, the equivalent static pressure was approximately one third of the maximum impact pressure.

Hinwood – Design for tsunamis – coastal engineering considerations – 2005

Sliding of tectonic faults in the ocean is the main origin of tsunami waves. Although it is not very likely to experience tsunami waves on the Texas or U.S. Atlantic coasts, it is possible. Searching on the NOAA/NGDC world tsunami database it can be seen that 12.2 m high tsunami waves were recorded on the coast of Portugal on November 1, 1755 (NOAA/NGDC, 2006). A tsunami wave with the same height was recorded on the coast of Ireland on November 21, 1894. Hinwood indicates that neglecting the small loss of energy with distance travelled by a wave, results in a small wave height reduction. In deep water a small tsunami travels at the speed:

$$c = \sqrt{gd} \qquad \text{Equation 62}$$

where g is the acceleration of gravity and d is the ocean depth. In mid ocean with depths of 16,400 ft, c = 500 mph, and for a typical shore depth of 164 ft, c = 50 mph. The author presents an analysis of wave forces on coastal structures, using the same equations given by Bea et al. (Bea et al., 1999). The horizontal force contains a hydrostatic component, owing to water gradients at both sides of the structure. The horizontal force also has a drag, impact, and inertia components. The vertical force has three components: a buoyancy term, a vertical dynamic lift force term, and a negative term (downward force) owing to the weight of water trapped on the structure after the wave passes (Hinwood, 2005).

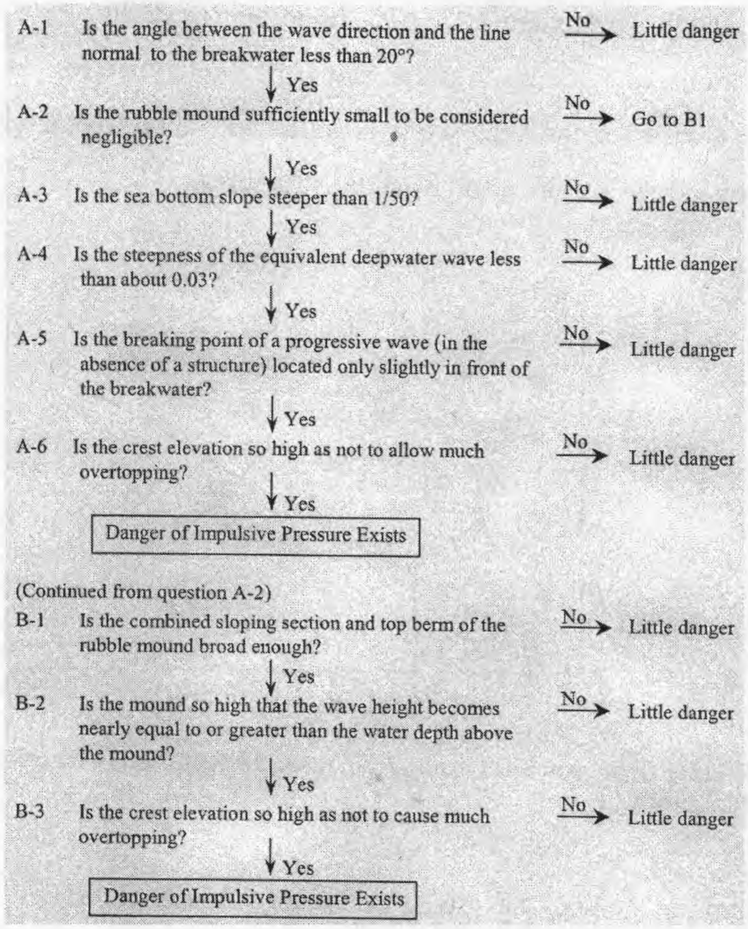

Figure 15. Questionnaire to evaluate the danger of impulsive wave pressure, source: (Goda, 2000).

Faltinsen – Sea loads on ships and offshore structures – 1990

Faltinsen indicates that the significant wave height can be larger than 2 m for 60% of the time in the North Sea area (Faltinsen, 1990). Wave heights larger than 30 m are possible. The mean period can range from 15 to 20 sec in extreme weather conditions and is seldom below 4 sec. The author points out that viscous effects and potential flow effects may be important in the determination of the wave induced motions and loads on maritime structures. Figure 16 can be used to make quick estimates as to when viscous effects and different potential flow effects are important. Regarding engineering tools, model tests are shown to have problems with scaling test results, while computer programs are having an important modelling role in calculating wave induced motions and loads on ships and offshore structures. However, the author indicates that more theoretical work is still needed on separated viscous flow and extreme wave effects on ships and offshore structures.

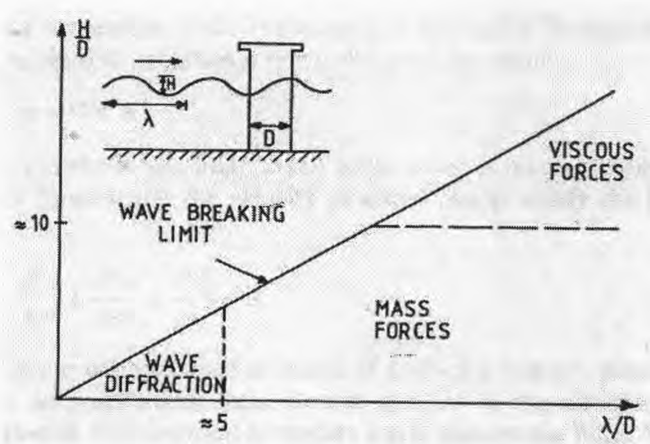

Figure 16. Relative importance of viscous drag, mass, and diffraction forces on marine structures, source: (Faltinsen, 1990).

Faltinsen studied the effects of water impact. He states that the duration of slamming pressure is in the milliseconds range. The slamming pressure is highly localized, and the position where high slamming occurs changes with time. The author presents a derivation to obtain a slamming pressure for a circular cylinder impacting a body of water at rest. Assuming irrotational flow and incompressible fluid he presents an equation for the hydrodynamic pressure and finds a slamming coefficient to be equal to π. However, the author reports that an experimental study by Campbell and Weynberg reports a value of 5.15 at the time of impact (Campbell and Weynberg, 1980). The author indicates that it may be valid to use only a fraction of the slamming loads because, the derivations presented assumed fluid incompressibility, and when compressibility is accounted for, the pressure has a peak value. This rationale is supported by the work of Hagiwara and Yuhara, where the authors indicate that the peak value of the slamming pressure gives a conservative estimate of the load distribution in

Kaplan – Wave impact forces on offshore structures – 1992

Kaplan presents a theoretical method to predict forces on horizontal cylinders and on flat plate decks (Kaplan, 1992). For a horizontal cylinder Kaplan proposed to estimate the vertical force per unit length of cylinder with the expression:

$$F_z = \rho g A_i + (m_3 + \rho A_i)\ddot{\eta} + \frac{\partial m_3}{\partial z}\dot{\eta}^2 + \frac{\rho}{2}\dot{\eta}|\dot{\eta}|d\left(\frac{z}{r}\right)C_{Dz}\left(\frac{z}{r}\right) \qquad \text{Equation 63}$$

where,

F_z = Vertical force per unit length

ρ = Water density

g = Acceleration of gravity

A_i = Immersed cross sectional area of the cylinder

m_3 = Vertical added mass

z = Immersed depth of cylinder

$\dot{\eta}$ = First derivative of wave crest elevation with respect to time

$\ddot{\eta}$ = Second derivative of wave crest elevation with respect to time

r = Radius of cylinder

d = Cylinder diameter

C_{Dz} = Drag coefficient for vertical flow (varies with immersed depth of the cylinder)

Figure 17 illustrates the definitions used by Kaplan for z, r, A_i, H, and η used in Equation 63.

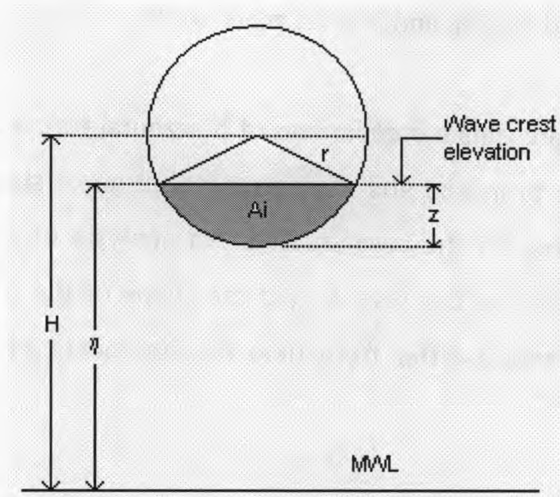

Figure 17. Definitions of z, r, A_i, H, and η.

The first term in Equation 63 is the buoyancy force, the term $\rho A_i \ddot{\eta}$ is due to the effect of the spatial pressure gradient in the waves, the terms including m_3 are obtained from the time rate of change of vertical fluid momentum, the last term is the drag force component.

The horizontal force produced on a cylinder by waves is given by:

$$F_y = (\rho A_i + m_2)\dot{v} + \frac{\partial m_2}{\partial z}\dot{\eta}v + \frac{\rho}{2}v|v|h\left(\frac{z}{r}\right)C_{Dy}\left(\frac{z}{r}\right) \qquad \text{Equation 64}$$

where,

m_2 = Horizontal added mass (depends on the level of immersion)

v = Horizontal wave orbital velocity

h = Cylinder diameter

C_{Dz} = Drag coefficient for lateral flow (varies with immersed depth of the cylinder)

Kaplan also proposes the following expression to be used to compute the vertical impact force acting underneath a flat rigid deck of negligible thickness:

$$F_z = \left(\rho\frac{\pi}{8}c^2\ddot{\eta} + \rho\frac{\pi}{4}\dot{\eta}c\frac{\partial c}{\partial t} + \frac{\rho}{2}\dot{\eta}|\dot{\eta}|cC_D\right)b \qquad \text{Equation 65}$$

where c is the wetted length, and b is the plate width.

The author presents a comparison of horizontal forces obtained from an analysis using the equations proposed and measurements at an offshore test structure, showing reasonable agreement for the case studied. An analysis of the vertical force on a flat plate presented by the author reveals that the shape of the force time history obtained using Equation 65 might differ from field measurements having high negative impact pressures.

Overbeek and Klabbers – Design of jetty decks for extreme vertical wave loads – 2001

A paper written by Overbeek and Klabbers examines the design of two jetty platforms built on the island of St. Vincent in the Caribbean. One was a container jetty, placed 8.2 ft above the still water level, and the other was a cruise berth, placed below the maximum expected hurricane wave level (Overbeek and Klabbers, 2001).

The authors conducted a literature search for design considerations, from which they decided to use two design equations for the projects.

For the impact pressure, assumed over the first 3 ft of the wave front:

$$P_{ve} = c\rho g H_{\max} \qquad \text{Equation 66}$$

For the slow varying pressure, assumed acting over the immersed portion of the structure:

$$P_{ve} = 1.0\rho g\left(H_{cr} - d_c\right) \qquad \text{Equation 67}$$

where,

P_{ve} = Vertical wave pressure

c = Wave impact constant, the authors used a value of 1.5

ρ = Specific density of water

g = Acceleration of gravity

H_{max} = Maximum wave height

H_{cr} = Wave crest above still water level

d_c = Height of the bottom of the deck above still water level

Equations 66 and 67 evolved from the fact that the pressure induced by waves varies as sketched in Figure 18. In order to avoid air entrapment the authors designed the cruise berth decks with the beams running only parallel to the berthing line, to avoid the entrapment of the waves in a beam grid. They also placed gaps in the deck in the transverse direction 2 in. wide every 6.5 ft. These gaps were covered with unanchored T-shaped timber strips to allow them to be blown out in the presence of the design waves.

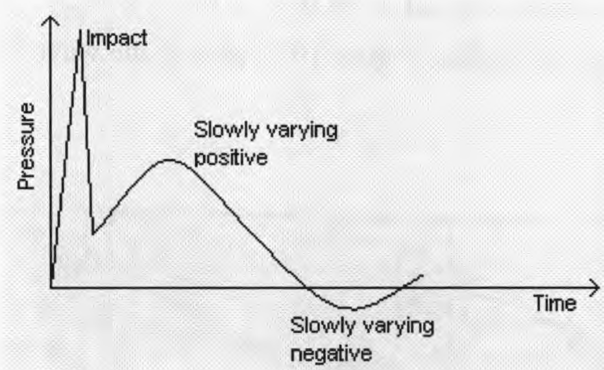

Figure 18. Wave induced pressures.

When Lenny, a category 4 hurricane, hit the cruise berth the authors concluded that design wave conditions were met. Although some structural damage was done, the structure could be easily restored. Some lightly anchored slabs were washed away by the storm. The authors estimated the pressure that caused the slabs to be detached from the structure was produced by an impact factor, c, of 3 or higher.

Chan et al. – Breaking-wave loads on vertical walls suspended above mean sea level – 1995

A laboratory experiment conducted by Chan et al. at the Hydraulics Laboratory in Singapore examined the forces produced by plunging waves on a suspended vertical wall. The authors intended to explore the impact pressures produced by breaking waves on suspended structures, such as facial beams of piers and wharves. The authors emphasize that extension of the design methodology used in the Shore Protection Manual (now Coastal Engineering Manual) for surface-piercing vertical walls to suspended structural elements would be inaccurate due to a significant difference in wave-structure interactions during wave action. The authors produced three types of waves during the experiment: (1) waves with an inclined wave front prior to jet formation, (2) an almost vertical wave front at the start of jet formation, and (3) a curved wave front after jet formation. Figure 19 illustrates the wave profiles as they impact the suspended wall.

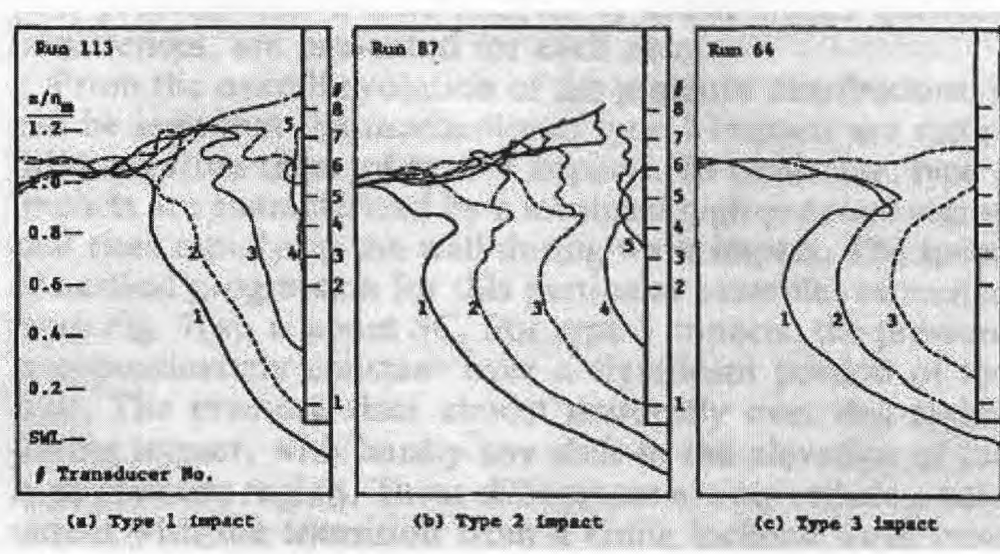

Figure 19. Incident wave profiles, source: (Chan et al., 1995).

On the right of Figure 19 a scale indicates the location of 8 sensors used on the hanging wall to measure wave pressures for each wave profile. Figure 20 shows the simultaneous records captured at the 8 sensor locations at impact.

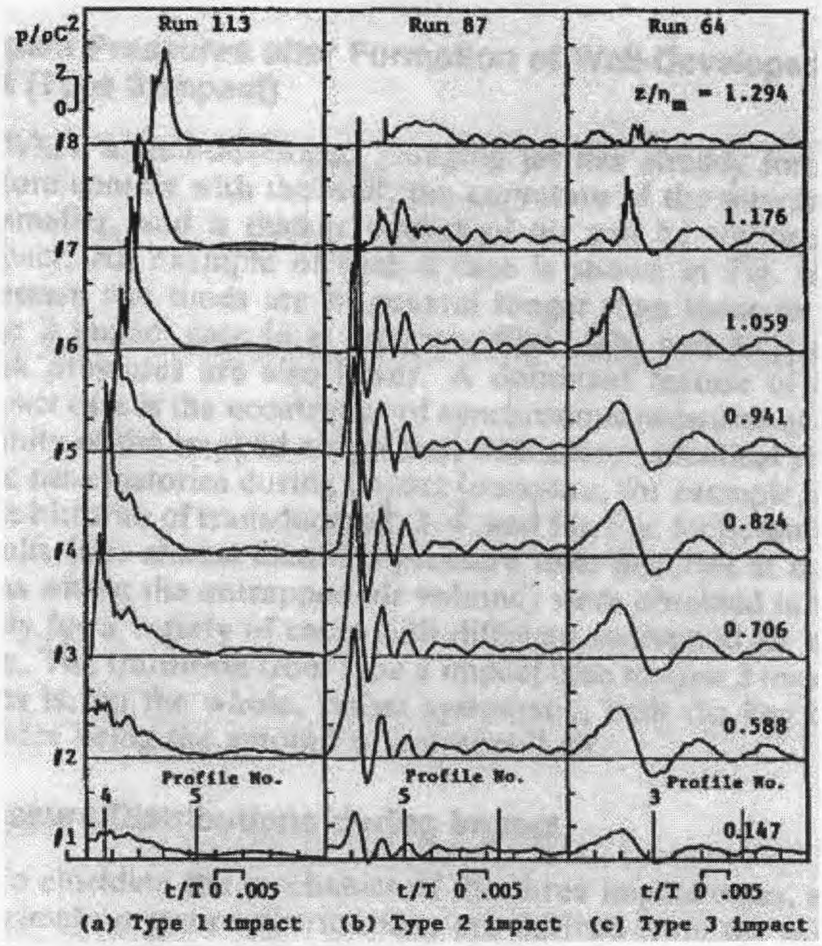

Figure 20. Three examples of simultaneous pressure records at impact, source: (Chan et al., 1995).

The records shown in Figure 20 indicate that the type I impact wave generates maximum pressures on the order of 10 ρC^2, where ρ is the density of water, and C is the characteristic phase speed of incident waves. Similarly, the type II impact wave produces maximum pressures of 12 ρC^2. While the type III wave impact generates maximum impact pressures of approximately 4 ρC^2. Although wave profile type I produces large pressures, the largest forces produced by this wave profile are approximately 3 $\rho C^2 \eta_m$, where η_m is the maximum crest elevation of a plunging wave in the absence of the wall. A similar value was obtained for the total force generated by the wave profile type III. Wave profile type II, however, produced a much larger force, namely 7 $\rho C^2 \eta_m$. This behavior is explained by the following reasons: wave type I produces large pressures, but since the peak pressures at different heights of the wall (sensor locations 1 through 8) are asynchronous, the resultant peak force is not very large. Wave profile type II produces large pressures simultaneously on most of the wall surface, thus generating the largest peak force. Wave profile type III generates synchronous peak pressures on most of the wall surface, although their magnitude is low due to cushioning of the pressure by large amounts of entrapped air between the plunging wave and the wall. A time history of the three impact forces on the wall is depicted in Figure 21.

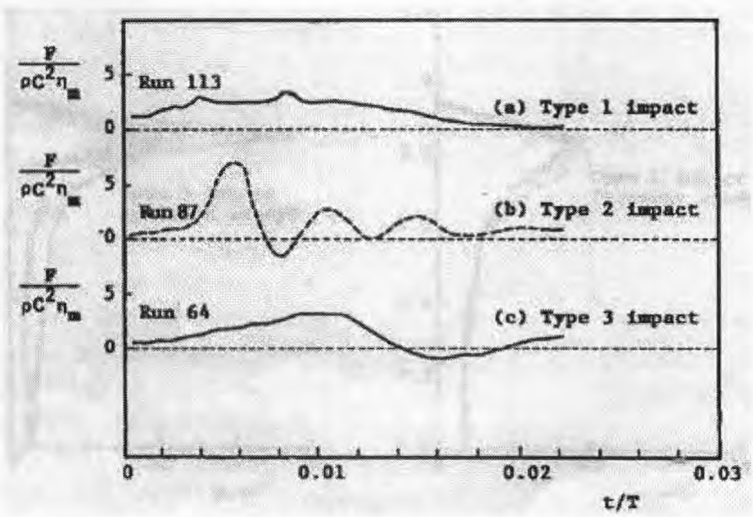

Figure 21. Horizontal force time histories, source: (Chan et al., 1995).

Pressure distributions captured along the wall height are presented in Figure 20. The pressure distributions suggest that the impact is more impulsive over the upper half of the wall; that is the region spanning from incident crest level to 0.5 η_m. The ordinates of Figure 22 indicate the distance above still water level, z, as a fraction of the maximum crest elevation, η_m.

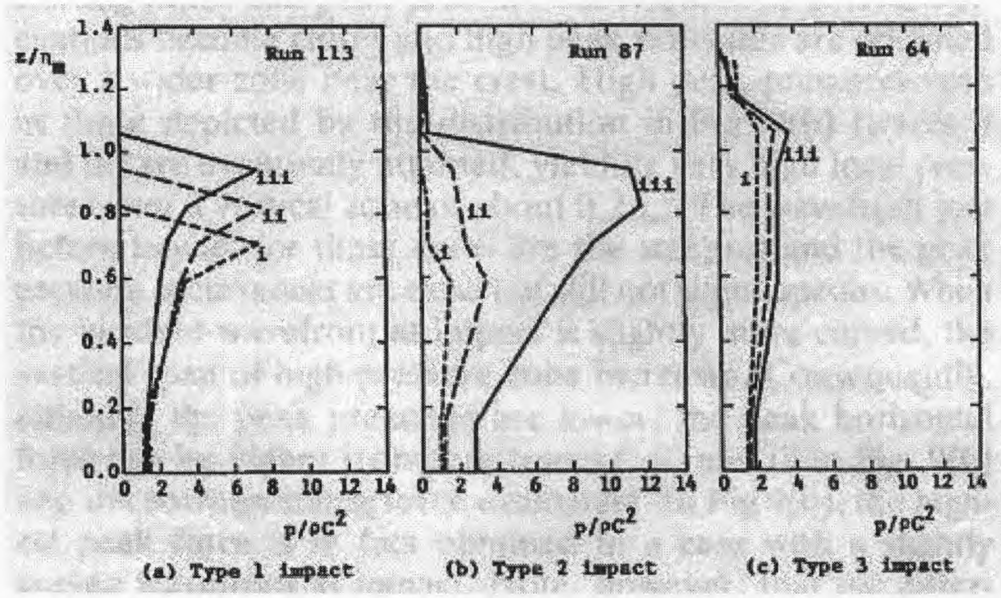

Figure 22. Sequential evolution of pressure distributions (i, ii, iii) for the three types of wave impact profiles, source: (Chan et al., 1995).

Weggel – Discussion of paper: breaking-wave loads on vertical walls suspended above mean sea level – 1997

Weggel presents experimental results similar to those reported by Chan et al. (Weggel, 1997). Weggel also presents a model for the pressure distribution on a vertical suspended wall as depicted in Figure 23. The author assumes the pressure distribution to be parabolic and concentrated near the wave crest. The pressure is zero at the wave crest, increasing parabolically downward, with the maximum pressure point located at a distance of 80% of the wall's height, above the bottom. The pressure distribution proposed is zero at and below 60% of the wall's height.

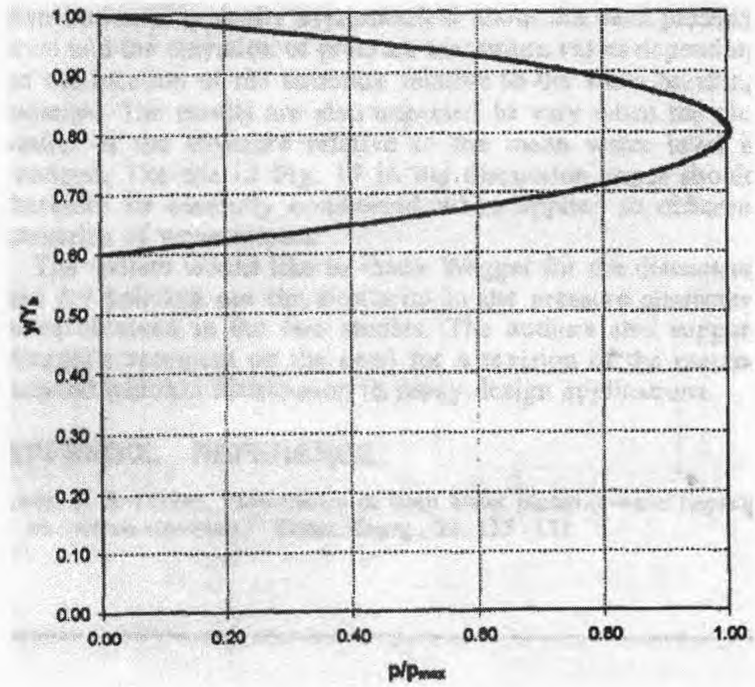

Figure 23. Pressure distribution on a vertical wall due to wave impact suggested by Weggel, source: (Weggel, 1997).

Aagaard and Dean – Wave forces: data analysis and engineering calculation method – 1969

The paper presents a method to compute wave forces on offshore structures (Aagaard and Dean, 1969). The authors use Morison's equation to compute the forces on the cylindrical elements of the platform. Once the design wave is defined in terms of wave height, wave period, and water depth, the authors calculate the kinematic flow field using a stream function to represent nonlinear ocean waves proposed by Dean (known as stream function theory). The authors used measured wave force and wave profile data and used the mathematical model to find empirical coefficients for drag and inertia. These drag and inertia coefficients were obtained by correlating measured wave forces with computed instantaneous horizontal particle velocities and accelerations. The authors show that the inertia coefficient varies between approximately 1 and 1.6 for Reynolds numbers approximately between 1.8×10^4 and 2.0×10^6. The drag coefficient recommended for design has a constant value of 1.2 and 1.35 for in-line forces for Reynolds numbers below 2.0×10^5 and 0.55 above 6.0×10^6, and has a smooth variation in between. The authors mentioned that the values given are "representative of average wave forces and are used in calculating wave forces for wave heights ranging to near-breaking, for all wave periods, for all water depths, for all phase and elevation positions in the wave, and for all piling diameters commonly used in wave force calculations for offshore structures." The pipe diameters used in the study ranged from 2 ft to 4 ft and at water depths from 33 ft to 100 ft.

The wave force was estimated using a computer program. The authors indicate that it is common practice in the offshore industry to compute wave forces at a number of locations on the structure within the wave to allow for smooth interpolation. The computer output includes surface wave profile, local forces at predetermined elevations and phase positions, and total force and moment about the base of the structure. The authors indicate that calculated distributed forces and average measured values agree within ± 10%. The authors indicate that other mathematical models may yield different drag and inertia coefficients yet produce valid computed forces.

Tickell – Wave forces on structures – 1993

Tickell summarizes information available to obtain design forces for coastal structures (Tickell, 1993). The author states that the design may use deterministic (long-crested regular) waves, but storm waves are random and short crested. The author presents a derivation of Morison's equation applied to slender cylinders where *D/L* is less than 0.2, indicating that for higher ratios of *D/L* diffraction effects are important. Where *D* is the diameter of the cylinder and *L* is the wavelength. The hydrodynamics of wave-current interaction cited by Tickell include studies by Hedges and Barltrop et al. (Hedges, 1987; Barltrop et al., 1990). When a current acts on the structure, the drag and inertia coefficients need to be modified. Tickell ends the chapter with a summary of wave loading on walls. The author points out that a useful method to compute non-breaking wave forces on vertical walls is described in the Shore Protection Manual (SPM, 1984) assuming a pressure distribution shown in Figure 24. The incremental pressure at the sea bottom is equal to

$$p_1 = 0.5\left(1 + H_r / H_i\right)\rho g\, H_i / \cosh(kd) \qquad \text{Equation 68}$$

where H_r is the reflected wave height and, H_i is the incident wave height.

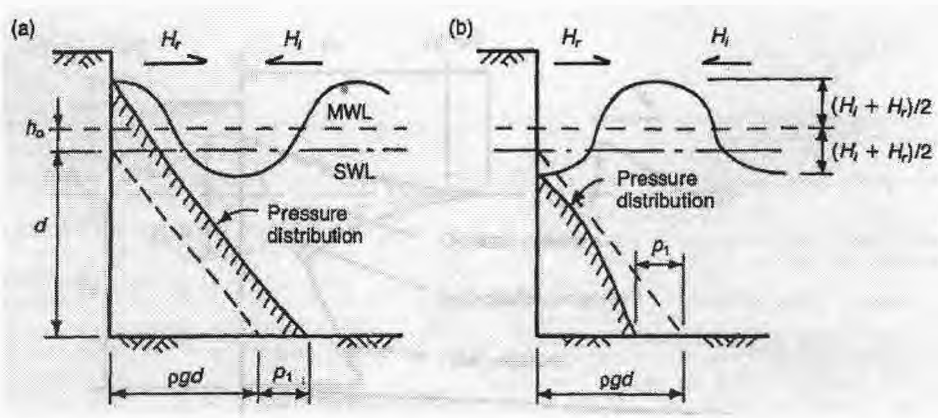

Figure 24. Non-breaking wave forces on a vertical wall (a) crest on wall (b) trough on wall, source: (Tickell, 1993).

For breaking waves Tickell suggests the use of the procedure followed by the Shore Protection Manual, based on Minikin's method, assuming the pressure distribution indicated in Figure 25. The dynamic pressure component is given by:

$$p_m = 0.5 C_i \rho u_b^2 \qquad \text{Equation 69}$$

where u_b is the characteristic velocity of the breaking wave and C_i is an impact coefficient.

It should be mentioned that Minikin's method is no longer recommended in the Coastal Engineering Manual, since it is considered to yield overconservative estimates of wave pressures.

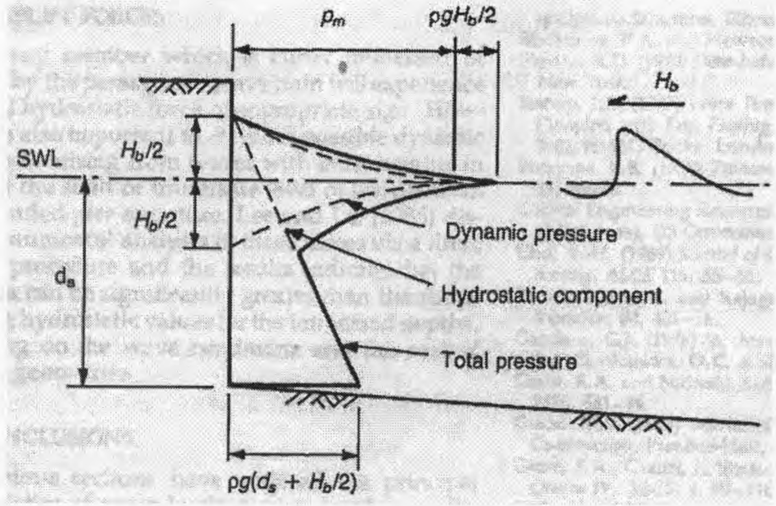

Figure 25. Breaking wave forces on a vertical wall, source: (Tickell, 1993).

For broken waves, the author describes the method used by the Shore Protection Manual, giving a dynamic pressure on the wall of:

$$p_m = 0.5\rho c^2 \qquad \text{Equation 70}$$

where c is the wave celerity. The dynamic pressure is assumed to act uniformly from the still water level (SWL) to $h_c = 0.78\ H_b$, where H_b is the height of the breaking wave. To this dynamic pressure a hydrostatic pressure distribution is added having a zero value at h_c above SWL and a pressure of $\rho g(h_c{+}d_s)$ at the sea bed, where d_s is the depth of water at the wall.

Denson – Wave forces on causeway-type coastal bridges – 1978

Due to observed damage caused by hurricane Camille to the Bay St. Louis and Biloxi Bay bridges, Denson initiated research on the effects of wave forces on bridge superstructures (Denson, 1978). Denson noted that hurricanes could produce extreme wave forces due to a general rise in water elevation (storm surge) accompanied by superimposed surface waves. Denson noted that perhaps most of the damage to the two bridges mentioned was due to vertical forces that exceeded the weight of the bridge superstructure. The effects of horizontal drag forces were evident in horizontal displacement of bridge sections on the Biloxi Bay Bridge. It is mentioned that bridge retrofit required extensive repairs. Another problem was anchorage failure at the superstructure-substructure connection. Denson built a 1:24 scale Plexiglass model of the bay St. Louis Bay Bridge. The bridge model was subjected to trochoidal waves with a period of 3 seconds. However, no further details on the wave type and the reason for using a period of 3 seconds are given in the report. Isaacson and Sarpkaya indicate that the physical realization of trochoidal waves seldom occurs. Isaacson and Sarpkaya state that an example of the development of a trochoidal wave is when waves are progressing against a wind that induces a vorticity within the fluid in the opposite sense of the particle motions (Issacson and Sarpkaya, 1981). The angle of wave attack in Denson's model was 90° (direction of wave propagation normal to bridge longitudinal axis). The author presented the results of the tests in dimensionless format. Five incremental test values were used for water depth. Five wave heights were used for each test condition, with heights ranging from nearly zero to breaking height. Five different deck clearances were also investigated, ranging from submerged-deck to deck placed above still water level. The results are presented for three different quantities per unit length of bridge, namely: rolling moment, lift force, and drag force.

Rolling moment per unit length

From the results presented it can be observed that overturning moments tend to be higher for deck locations near or below the surface water level than for decks placed above the water level. As the value of the variable h/W (ratio of bridge deck height measured from sea bottom to deck width) decreases (as the deck is located closer to the sea bottom), there is no discernible difference between the moments measured for different values of the h/D variable (ratio of bridge deck height measured from sea bottom to water depth).

Lift force per unit length

For high values of the h/W variable the lift forces are lower for decks placed above water level than for decks placed near or below water level. As the variable h/W is reduced, the lift force is reduced with respect to values measured for high values of *h/W*. For example, if the *h/W* values are reduced from 0.64 to 0.38 the lift force is reduced to approximately 60%. As the variable *h/W* increases, the lowest lift force values are obtained at elevated decks.

Drag force per unit length

By reducing *h/W* from 0.64 to 0.38 the drag force is also reduced to approximately 60%. That is, the drag force is reduced as *h/W* is reduced. The moment, lift, and drag forces always increase with increasing values of the wave height to water depth ratio. The lift force tends to be between 5 and 7.5 times the value observed for the drag force.

The tests were conducted on two sets of bridge decks consisting of seaward and landward lanes supported independently. Since the waves were moving from sea toward land, the moment, lift, and drag forces in general, tend to be smaller for the landward sections, with some exceptions. The moment and lift force values recorded for landward sections were approximately 75% of those observed on the seaward sections.

Design procedure

Denson proposed the following design method using his results:

1. Define the bridge geometry and height above sea bottom.
2. Estimate the maximum water depth including storm surge.
    a. The previous two steps define *h/W* and *h/D*.
3. Find the maximum value of moment, lift, and drag from the figures presented in the report, using a value of wave height to water depth ratio of 0.7.

Figure 26 shows a typical plot of the results presented in the report. The quantities *h/D* and *h/W* have been defined before, and *r* is the correlation coefficient obtained using a least square approximation with a third degree polynomial. *H/D* is the ratio of wave height to water depth, and the overturning moment, *M,* is nondimensionalized by dividing it by the specific weight of water, γ, and by the width of the bridge deck, W, raised to the third power. In this case M has units of *lb-ft/ft*, γ has units of lb/ft^3, and W has units of *ft*.

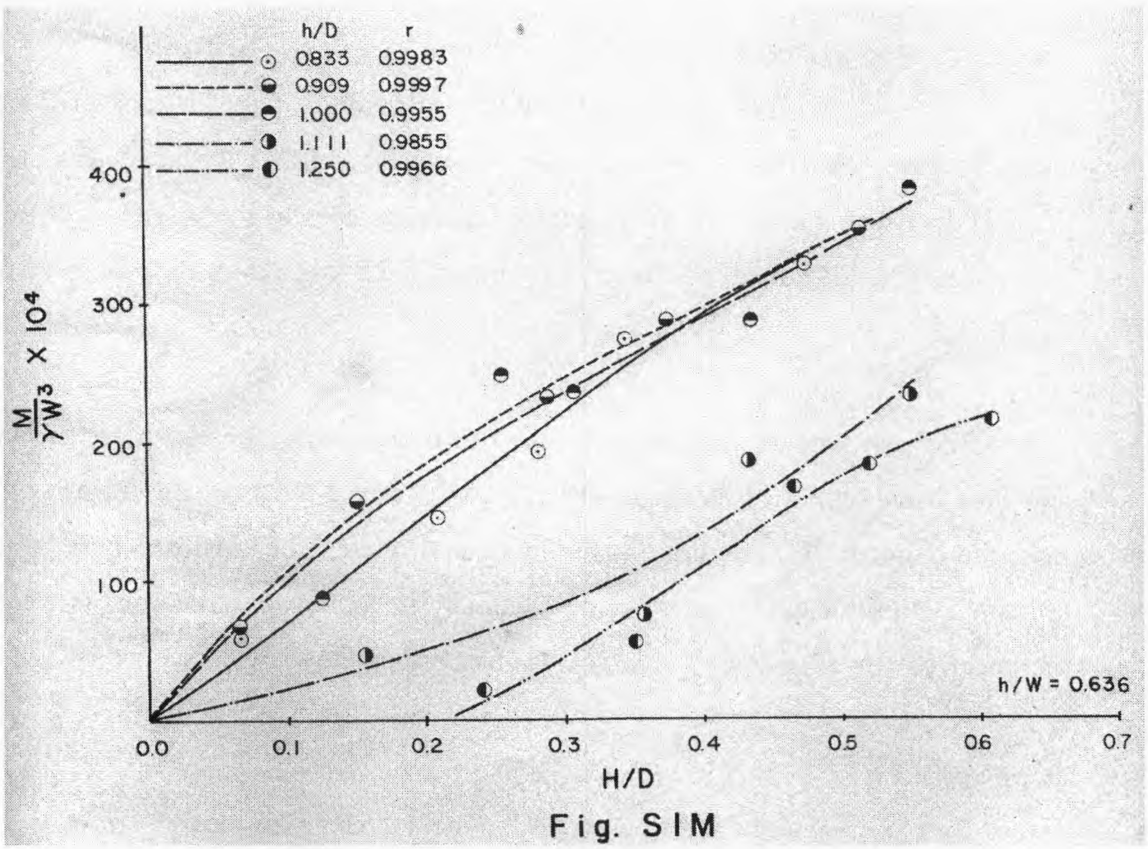

Figure 26. Results for overturning moments, *M*, of seaward deck under condition 1, source: (*h/W* = 0.636), (Denson, 1978).

Denson – Wave forces on causeway-type coastal bridges: effects of angle of wave incidence and cross-section shape – 1980

The author carried out a set of tests on two model specimens of bridge sections. One was a model scaled to 1:24 of the Bay St. Louis Bridge located in Mississippi on U.S. Highway 90, heavily damaged by hurricane Camille in 1969, which developed a storm surge of nearly 20 ft. The bridge consists of two separate bodies (seaward and landward), each having a 48 ft span and a two-lane beam and slab cross-section with four beams each. The width of the deck, *W,* of this study refers to the width of a two-lane section supported by four beams. The other was a trapezoidal box girder section built to a 1:24 geometric scale. The bridges were fixed in a tank at a constant height above the floor, subjected to waves with a period of 3 seconds. The bridge sections were supported on piles to simulate bridge conditions and subjected to waves of five different heights, using five different mean water levels. The bridge models were tested under five different angles of wave attack (angle between longitudinal axis of bridge and direction of wave travel), namely: 30°, 45°, 60°, 75°, and 90°. The following quantities were measured: rolling, pitching, and yawning moments, a well as transverse and longitudinal drag forces, and lift forces.

The author includes a section in which he describes a survey being given to bridge engineers in 22 states. Out of 20 states replying, 6 reported damage observed on coastal bridges, and 17 states reported bridges located in areas susceptible to damage. After the questionnaire was received, two bridges were destroyed by hurricane-type waves and winds: the Hood Canal floating bridge in Washington and the Dauphin Island causeway in Alabama. The Hood Canal floating bridge was damaged in 1979 by a cyclone with average winds of 80 mph and wind gusts of 115 mph. Dauphin Island causeway lost many spans to hurricane Frederic in 1979 with recorded wind gusts reaching 145 mph and an estimated storm surge of 13 ft. The damaged caused on the St. Louis Bay Bridge and Dauphin Bay Bridge was horizontal transport due to hydrodynamic lifting and dragging forces.

Denson makes a more detailed description of the method used to measure the waves and forces than used in his 1978 study. The author describes the design method that could be followed using his report, which is essentially the same method described for the 1978 report. There are some differences between this project and the 1978 study. The model with slab and beams used in this study has end diaphragms, while the model used in the 1978 study did not have end diaphragms. This fact is not specified in the 1978 document. The forces reported in the 1978 study are given in units of force per unit length, while the forces in this study are given in units of force. The 1980 study makes a comparison of the two studies by listing maximum measured lift and drag forces, as well as overturning moments for the 90 incidence waves. However, the results presented in the report could not be verified from the information given on the plots where they were extracted, neither for the 1978 study nor for the 1980 study.

The report compares the values of the vertical lift force obtained for the slab-beam bridge with the box-girder bridge. The values for the seaward bridge sections of the non-dimensionalized lift force coefficients ($Fz/\gamma W^3$) are summarized in Table 4. The lift force, Fz, has units of *lb*, the density of water, γ, has units of lb/ft^3, and the width of the bridge, W, has units of *ft*. The values of the lift force coefficients presented in the comparison given in the report are different from the values read from the plotted results shown in appendices B and C of the report. Thus, the values given in Table 4 are those obtained directly from the appendices.

Table 4. Values of coefficient Fz/GW^3x10^3 for different angles of wave incidence

Angle of incidence	Slab-beam bridge		Box girder bridge	
	Positive	Negative	Positive	Negative
30°	183	128	307	Negligible
45°	237	149	392	
60°	184	165	469	
75°	267	156	548	
90°	267	146	857	

Table 4 shows that the negative force coefficients are nearly independent of angle of wave incidence. The lift force magnitude increases for the box girder section as the angle of wave incidence approaches 90°. However, no conclusions can be drawn for the lift force acting on the slab-beam bridge section. Denson mentions that in order to compare the values of the slab-beam section with the box girder section the slab-beam values need to be multiplied by two to account for span length. The report indicates that doing that elicits a similar behavior between the box girder section and the slab-beam section. However, that could not be verified using the values from Table 4.

Wang – Water wave pressure on horizontal plate – 1970

The paper is mainly concerned with the uplift pressure induced by waves on the underside of a horizontal plate placed either at mean water level or above mean water level. The author asserts that the uplift pressure has a slowly varying component and an impact component. The author explains that the impact pressures produced by waves as they come in contact with horizontal and vertical barriers are different. It is pointed out that the impact on the underside of a deck is produced by the change of momentum of the fluid flow. While the impact produced on a vertical wall is produced by the collapse of an air layer. Wang presents a set of equations for a standing wave system (waves typically generated by wind). The author used the assumption proposed by von Kármán, that affirms that the mass responsible for impact under a flat plate fixed near the water surface is the mass of water enclosed in a semi-cylinder of diameter, 2*S*, and length, *b*, as depicted in Figure 27.

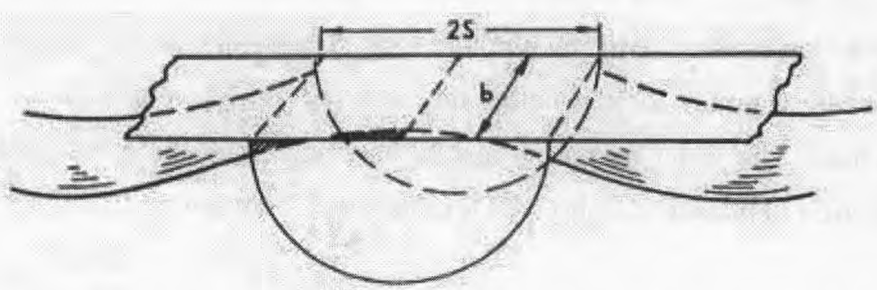

Figure 27. Profile of standing wave modified after contact with a horizontal flat plate, source: (Wang, 1970).

The impact pressure computed is given by:

$$\frac{p_i}{\gamma} = \frac{\pi}{2g} v^2 \delta \qquad \text{Equation 71}$$

where,

p_i = Impact pressure

δ = Factor that depends on the shape and degree of asymmetry of the incident wave

γ = Specific weight of water (lb/ft^3)

g = Acceleration of gravity (ft/sec^2)

v = Vertical velocity of water particles at the surface of the plate (ft/s)

The author carried out a series of experiments in a 90 ft square basin. By inserting a plunger into the water, and by retrieving it out of the water, dispersive waves were generated for the tests. The waves generated by this method are akin to dispersive waves produced by an explosion rather than to standing waves generated by wind during a storm. As such, the period and wave length of the dispersive waves generated were variable and difficult to measure. The plate was placed at several distances from the water surface that ranged from 0 to 1.5 in.

It was observed that the wave pressure depends on the characteristics of the wave at the moment of impact. Impact pressures are likely to be produced by waves of moderate steepness preceded by a trough located below the deck. Steep waves or waves preceded by a trough located below the deck are not likely to produce impact. After waves break, the water motion is mainly horizontal, and the uplift pressure is nearly hydrostatic. No impact was observed for this wave condition.

The author compared measured pressures with the following equation derived to obtain impact uplift pressure induced by dispersive waves.

$$\frac{p_i}{\gamma} = \pi\left[1-\left(\frac{d}{T_r A}\right)^2\right]^{1/2} T_r A \tanh\sigma \qquad \text{Equation 72}$$

where,

p_i = Impact pressure

γ = Specific weight of water (lb/ft^3)

A = Wave amplitude

d = Clearance between still-water level and deck underside

σ = $2\pi h/\lambda$

h = Water depth

λ = Wave length

T_r = Transmissibility = H/H_I (Attenuation of incident wave height by the presence of the deck)

$$T_r = \frac{1}{\left\{1-\left[\frac{\pi B}{\lambda}\left(1-\frac{2d}{H_I}\right)\right]^2\right\}^{1/2}}$$ Equation 73

H_I = Height of incident wave (before reaching the plate)

H = Wave height at a given location landward of location where H_I was measured

B = Length of plate from leading edge to point where H needs to be determined

The experimental observations did not agree with predictions made by Equation 73 modified as shown below. Thus, upper bound values were proposed for the ordinate, Y, shown in Equation 74 by the author as 3.14 for a constant water depth study and 4.5 for shoaling water.

$$Y = \frac{p_i}{\gamma\left[1-\left(\frac{d}{T_r A}\right)^2\right]^{1/2} T_r A}$$ Equation 74

The durations of impact observed in the study varied from 6 msec to 16 msec, with an average of 11 msec. Measured slowly varying pressures were one to two times the hydrostatic pressure.

El Ghamry – Wave forces on a dock – 1963

The study by El Ghamry was one of the earliest of its type (El Ghamry, 1963). The author studied uplift pressures, uplift forces, reactions, and moments on a dock, induced by waves generated in a flume (105 ft long, 1 ft wide, and 3 ft deep). Fresh water was used in the experiments. The dock was made of aluminum and was 4 ft long, 1 ft wide, and ¼ in. thick. Several test cases were investigated by the author: one involved no breaking waves allowing an air gap underneath the deck, another case involved breaking waves with 1:3 and 1:5 beach slopes, some other variations with and without air gap under the deck were also studied. The waves used in the study were monochromatic with varying periods and heights.

The force and pressure records have a periodic shape that depends on wave period, T, and the deck clearance above the mean water level. The author made an attempt to predict the uplift pressures using Stoker's wave theory. However, since Stoker's theory predicts a sinusoidal shape for the waves, and the wave records were not symmetric, discrepancies were found. An approximation was, however, obtained for the uplift force and downward force using Stoker's theory by employing curve fitting to the data recorded and the parameters of Stoker's theory. The following equations resulted for uplift force and downward force, respectively, for the case of a deck placed at the still water level:

$$F_1 = C_1 C_2 \frac{\rho_f g \lambda H}{2} \qquad \text{Equation 75}$$

where,

F_1 = Uplift force

$$C_1 = \sqrt{1 + \frac{3r^2}{1+r^2}} \qquad \text{Equation 76}$$

r = $\pi\lambda/L$

and ρ_f is the mass density of the fluid, g is the acceleration of gravity, λ is the length of the dock, H is the wave height, L is the wave length, C_2 is a correction factor obtained from Figure 28, and

$$F_2 = C_4 \rho_f gHL \qquad \text{Equation 77}$$

where F_2 is a downward force, and C_4 is a function of wave steepness and can be obtained from Figure 29.

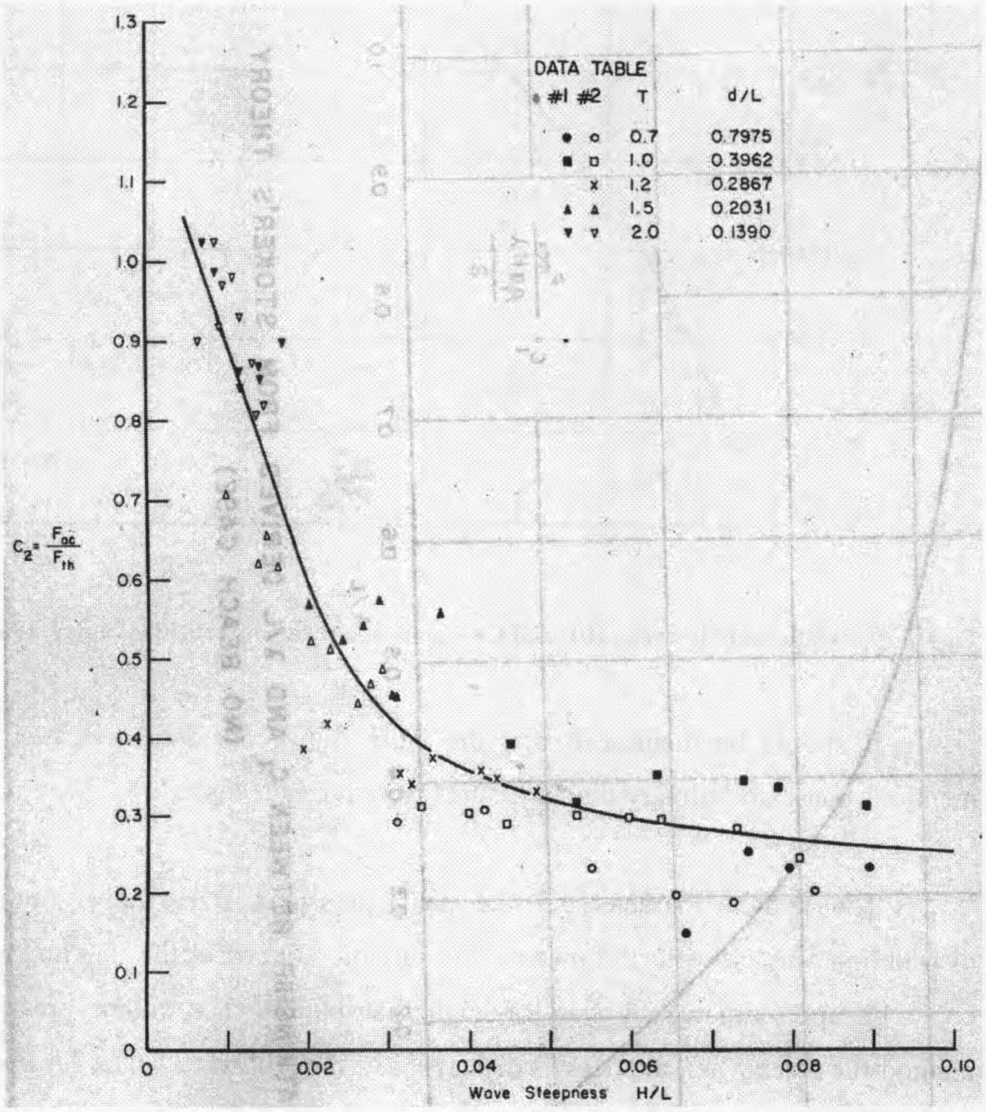

Figure 28. Relationship wave steepness and C_2 – no beach case, source: (El Ghamry, 1963).

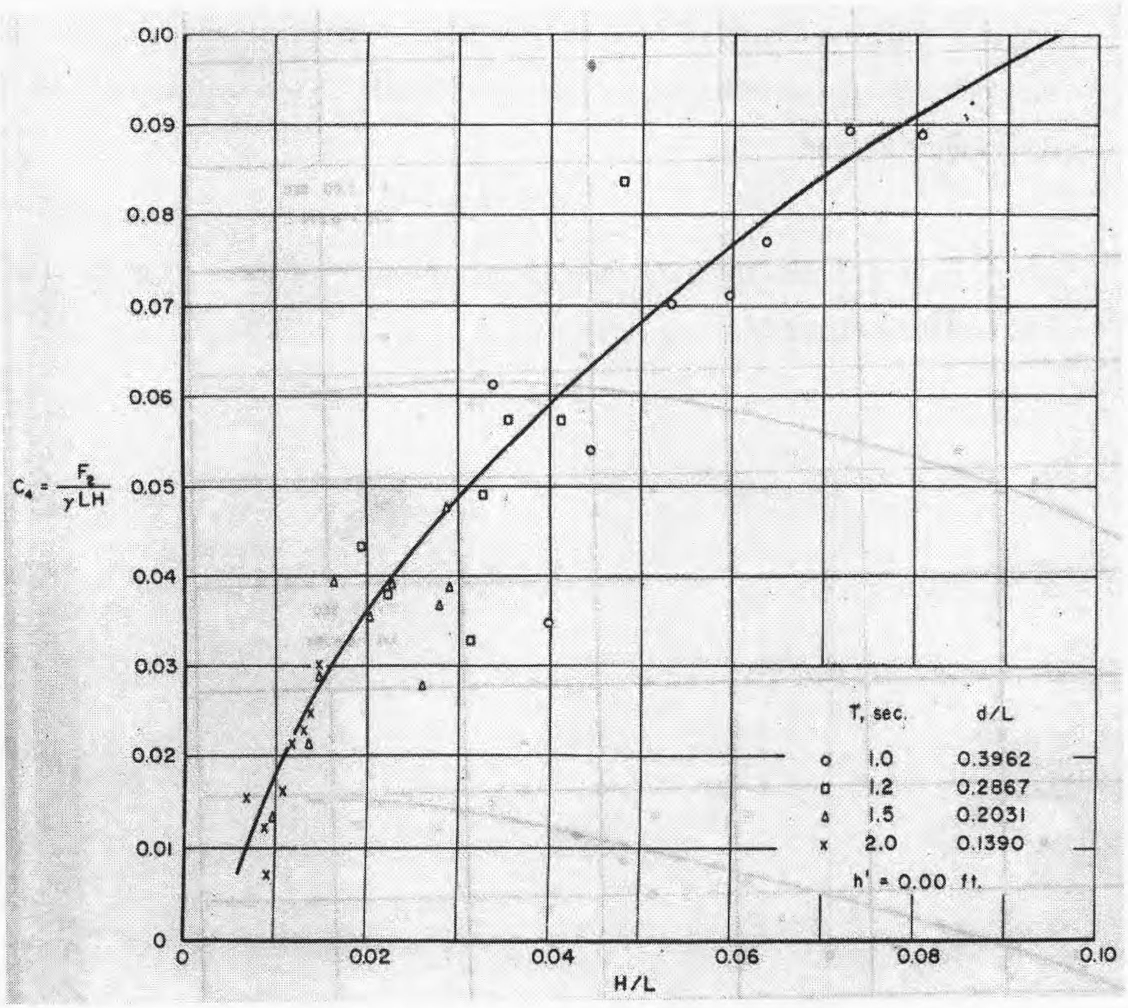

Figure 29. Relationship between H/L and C4 – no beach case, source: (El Ghamry, 1963).

It should be mentioned that the plots show considerable scatter. The author mentions that extraordinary high pressures were rarely recorded.

The author characterized the peak pressures statistically, finding that the distribution was close to the normal distribution. Likewise, the maximum uplift force could be approximated by the Rayleigh distribution. The author presents a design method for cases when the deck is placed above the still water level, for known incident wave characteristics. The author indicated that for the case when there was no air gap under the deck, the uplift force developed had an order of magnitude greater than for cases when there was room for the air to escape. On few instances the uplift force was as high as 100 times that of the no air entrapment case.

Douglass et al. – Wave forces on bridge decks – 2006

Douglass et al. carried out a literature review of wave forces on bridge decks, investigated the causes of failure of the U.S. HW 90 Bridge across Biloxi Bay after it was hit by hurricane Katrina, presented the results of some laboratory experiments, and proposed a method to estimate wave forces on bridge decks (Douglass et al., 2006). The researchers assumed the wave and surge conditions at the bridge site when hurricane Katrina crossed the area where as follows:

- Significant wave height $H_s = 6.2$ ft
- Wave period $T = 5$ sec
- Water depth $d = 16$ ft
- Storm surge $\overline{\eta} = 12$ ft

The authors presented an appendix with the computation of forces estimated by different methods available for a case study involving the failure loads of the bridge on U.S. HW 90, across Biloxi Bay. The authors computed the weight of the span to be 340 kips. The results presented by the authors are summarized in Table 5. The forces estimated by a method proposed by the authors are also included in Table 5.

Table 5. Summary of results obtained by Douglass et al.

Method	Uplift Force (kips)	Lateral Force (kips)
McConnel et al., avg. values, 2004	520	165
Bea et al., 1999	inertia + drag	inertia + drag + slamming
	320 + 130 = 450	430 + 40 + 250 = 720
Denson, 1978	50	9
Denson, 1980	710	150
Douglass et al., 2006	440	230

Our research team examined and verified most of the results. However, it can be noted that discrepancies between the results obtained by different methods are due to the geometry of the sections used to develop the equations. For example, the geometry used in Denson's study has a shallower section and less beams than the Biloxi Bridge, thus lower lateral force values are obtained from Denson's equations. It should be mentioned that the values reported by Denson's study are maxima, while the values computed by Douglass et al., when using McConnel et al.'s equations, are average (Denson, 1980; McConnel et al., 2004). For the results of both studies to be comparable, the values obtained using the McConnel et al. study should be multiplied by the coefficients for upper limit recommended by McConnel et al. (approximately 1.5 for vertical forces and 2 for lateral forces). It should be mentioned that the studies carried out by McConnel et al., El Ghamry, and Denson show considerable scatter in the data (McConnel et al. 2004; El Ghamry, 1963; Denson, 1980). The values computed by our research team using the equations given by some of the studies are presented in Table 6.

Table 6. Uplift force and lateral force estimated by various methods

Method	Uplift Force (kips)	Lateral Force (kips)
McConnel et al, upper values, 2004	568	165
Bea et al., 1999	inertia + drag	inertia + drag + slamming
	320 + 130 = 450	430 + 40 + 125 = 595
Denson, 1978	50	9
Denson, 1980	710	150
Douglass et al., 2006	440	230
El Ghamry, 1963	332	N.A.

An approximate analysis employing the study made by El Ghamry for the same bridge using the same wave conditions was made by our research team and is presented next (El Ghamry, 1963).

Equation 78 was needed to estimate uplift force for a deck placed above the still water level:

$$F_1 = C_1 C_2 C_3 \frac{\rho_f g \lambda H}{2} \qquad \text{Equation 78}$$

where,

λ = Length of dock (in our case width of deck) = 33.3 ft

ρ_f = Mass density of fluid = 2 slugs/ft^3

g = Acceleration of gravity = 32.2 ft/sec^2

L = Wave length = 104 ft (using same value estimated by Douglass et al.)

λ/L = 33 ft / 104 ft = 0.32, so from Figure 21 of El Ghamry, C_1 = 1.6

H/L = Wave height over wave length = 10.4 ft / 104 ft = 0.1, so from Figure 22 of El Ghamry, C_2 = 0.25

d/L = Water depth over wave length = 16 ft / 104 ft = 0.15

h' = 1 ft (Clearance between still water level and lower level of the deck)

$\Delta H'$ = $H/2 - h'$ = 10.4 ft /2 – 1 ft = 4.2 ft

$\Delta H' / H$ = 4.2 ft / 10.4 ft = 0.40, so from Figure 24 of El Ghamry, C_3 = 1.1

The values listed above were used in Equation 78 to give,

$$F_1 = (1.6)(0.25)(1.1)\frac{\left(2\,\frac{slugs}{ft^3}\right)\left(32.2\,\frac{ft}{\sec^2}\right)(33\,ft)(10.4\,ft)}{2}\left(\frac{52\,ft \cdot long}{1\,ft \cdot wide}\right) = 255 kips \quad \text{Equation 79}$$

Using a factor of safety recommended by El Ghamry of 1.3, the total uplift force was calculated to be: 255 * 1.3 = 332 kips. Equation 79 was multiplied by 52, the length of the Biloxi Bay Bridge and divided by 1 ft, the width of the dock used in El Ghamry's study. Notice that the model studied by El Ghamry did not have beams under the plate.

DESIGN GUIDELINES FOR WAVE FORCES ON BRIDGE SUBSTRUCTURE

The design of a bridge substructure spanning a body of water always accounts for water flow forces imposed on the substructure, and potential resulting scour. This section contains a brief description of current bridge design aids and specifications used in the design of bridge substructures subjected to water flow forces.

A critical aspect of the design of a bridge spanning a waterway is the design of the bridge substructure against scour and the design of the foundation to sustain forces from stream flow, debris, and ice. For this type of design there are a number of sources available, such as Chapter 7 of the Shore Protection Manual (SPM, 1984), Evaluating Scour at Bridges (FHWA, 2001), Stream Stability at Highway Structures (FHWA, 1991), Section 8.9 Bridge Scour of the TxDOT Hydraulic Design Manual (TxDOT, 1997). It is worth mentioning that scouring around the foundation of bridges is the most prevailing source of failure of bridges subjected to floods and other actions of water (Hamill, 1999).

Field inspection of the structure of bridges recently damaged by hurricanes show that bridge foundations were not a major source of damage. After being inspected by structural divers, it was concluded that the foundation of the bridge on I-10 across Lake Pontchartrain in New Orleans did not show scour problems although the superstructure was badly damaged by hurricane Katrina in 2005. A similar situation was identified during a field visual inspection by our research team to the bridge on U.S. highway 90 across St. Louis Bay in Mississippi. By inspecting photographs of the Biloxi Bay Bridge, the same observation can be made, since most of the piers remained vertical after hurricane Katrina struck the area.

Section 3.7.3.1 of the AASHTO Bridge Design Manual contains an equation to compute the stream pressure acting along the longitudinal axis of a pier (AASHTO 2004):

$$p = \frac{C_D V^2}{1000} \qquad \text{Equation 80}$$

where,

p = lateral pressure, *ksf*

C_D = drag coefficient for piers, depends on the shape of piers and whether debris is lodged against a pier, varies from 0.7 and 1.4

V = design velocity of water for the design flood in strength and service limit states and for the check flood in the extreme event limit state, *ft/sec*

Table 7 presents a list of some sources of information available for substructure design. The design of piers, abutments/retaining walls that transfer loads onto spread footings, driven piles, and drilled shafts and the water related forces acting on them are discussed in documents about substructure design (Anderson, 1995), publications of the Federal Highway Administration (FHWA, 2001; FHWA, 2004), and the Coastal Engineering Manual (CEM, 2006).

Table 7. Substructure design methods

Method	Description	Parameters	Reference
Stream Pressure	Method applies pressure $P = C_D V^2$ in the direction of flow against substructure.	P = stream pressure, C_D = drag coefficient, V = velocity of water.	(Xanthakos, 1995), p. 93
Scour	Method applies several equations toward designing bridges to resist scour.	Flood event, discharge, water surface profiles flood history, watershed characteristics, bridge location, and erosion history.	(FHWA, 2001)
Earth pressure due to ponding	Applies earth pressure, static water pressure, and passive pressure to retaining wall or abutment. Checks are made for sliding, overturning, and bearing capacity. Flow net analyses are employed.	Hydrostatic pressure, earth pressure.	(Xanthakos, 1995), p. 418
Uplift	Applies water table at the underside of superstructure (foundation submerged) and computes uplift based on the parameters listed.	Hydrostatic pressure, dead weight of superstructure and diaphragm walls, friction, pile, or shaft characteristics.	(Xanthakos, 1995), p. 433, 633
Breakwater design (buoyancy)	Applies wave pressure by striking waves to structures that are submerged.	Height of water, velocity of propagation, maximum velocity, empirical constant, acceleration due to gravity.	(Anderson, 1984), p. 254
Scour and scour depth	Presents design guidelines toward predicting different types of scour and scour depth.	Velocity of flow, channel characteristics, flow path, water level, river bed characteristics, pier configuration/inclination to flow, volume of debris.	(Xanthakos, 1995), p. 180
Shore protection (revetments)	Guidelines for using revetments.	Revetment type (rigid or flexible) water/wave height channel slope and characteristics.	(FHWA, 2004), p. 7.10

DESIGN GUIDELINES FOR WAVE FORCES ON BRIDGE REVETMENTS

A well-known source to verify the stability of channel revetments or to design channel revetments is the Coastal Engineering Manual of the U.S. Army Corps of Engineers (CEM, 2006).

III. CONCLUSIONS

This chapter describes the conclusions arrived at after analyzing the information found in the preparation of this document.

A verifiable method for design of the superstructure of coastal bridges that can withstand the action of wave forces is not currently available in the literature. A vast amount of information is available about waves and wave loading, but only two documents were specifically developed for coastal bridges (Denson, 1978 and Denson, 1980). El Ghamry presented one of the earliest studies, although it was developed for a dock (El Ghamry, 1963).

An important conclusion is that horizontal forces produced by waves acting on a bridge deck are smaller than vertical forces. Apparently horizontal pressures can be twice as high as the hydrostatic horizontal pressures, while vertical pressures can be approximately six times as high as vertical hydrostatic pressures (McConnell et al., 2004). However, El Ghamry reported that extraordinary high vertical pressures were rarely recorded (El Ghamry, 1963). El Ghamry also reported that the vertical pressure head reached values as high as 2.5 times the incident wave height but was typically less than that.

By reviewing the vertical and lateral force estimates obtained using the studies performed by Bea et al., 1999; Denson, 1978; Denson, 1980; El Ghamry, 1963; McConnel et al., 2004, and Douglass et al., 2006, we can observe significant discrepancies. Most of the methods predict uplift forces in excess of the 340 kips weight of the of the Biloxi Bay Bridge span, except for the study carried out by El Ghamry, which predicts force values slightly under the bridge weight.

A more detailed comparison of estimates of forces obtained from different methods should be done, since different methods made different assumptions and the experiments used to arrive at the various methods proposed involved structures with different characteristics. Some of the differences are attributed to the fact that some methods predict average force values, while others estimate maximum forces.

Most methods were not developed for bridge structures, which are unique in their design. Thus, new numerical or physical studies on typical bridge configurations are necessary to validate the force prediction methods proposed in the literature.

An investigation of the state of knowledge in design aids and codes showed that some documents account for the effects of wave-induced forces. However, none of the design aids reviewed proposes a method developed specifically to estimate wave forces on bridge decks.

All experimental reports presented great variability in the data obtained. In this regard, due to the uncertainties involved in the prediction of pressure imposed by waves on structures, the Coastal Engineering Manual proposes the designer to use the equations they provide as a preliminary estimate. The CEM recommends the final design of important structures to include laboratory tests. The CEM also states that no reliable method exists to predict impulsive pressures produced by breaking waves, due to the extremely stochastic nature of wave impacts. This shows the level of uncertainty involved in this type of environmental loading. Thus, the need of coastal engineering knowledge for the design of bridges is evident.

REFERENCES

Aagaard, P.M. and Dean, R.G., *Wave Forces: Data Analysis and Engineering Calculation Method*, Offshore Technology Conference, Dallas Texas, Paper No. OTC 1008, pp. I95-I107, 1969.

AASHTO, *LRFD Bridge Design Specifications*, Customary U.S. Units, Third Edition, 2004.

Anderson, P., *Substructure Analysis and Design*, Ronald Press, 1995.

ASCE/SEI 7-05, *Minimum Design Loads for Buildings and Other Structures*, ASCE Standard, American Society of Civil Engineers, 2006.

ASCE/SEI 24-05, *Flood Resistant Design and Construction*, ASCE Standard, American Society of Civil Engineers, 2006.

Barltrop, N.D.P., Mitchell, G.M., and Atkins, J.B., *Fluid Loading on Fixed Offshore Structures*, UK Department of Energy, OTH 90 322, 2 Volumes, HMSO Books, London, 1990.

Bea, R.G., Xu, T., and Ramos, R., *Wave Forces on Decks of Offshore Platforms*, Journal of Waterway, Port, Coastal, and Ocean Engineering, May/June 1999, pp. 136-144.

CALTRANS, *Bridge Design Specifications*, California Department of Transportation, http://www.dot.ca.gov/manuals.htm, Accessed on March 19, 2005.

CALTRANS 2005a, *Bridge Design Practice*, California Department of Transportation, 2005, http://www.dot.ca.gov/manuals.htm, Accessed on March 19, 2005.

CALTRANS 2005b, *Bridge Design Aids*, California Department of Transportation, 2005, http://www.dot.ca.gov/manuals.htm, Accessed on March 19, 2005.

CALTRANS 2005c, *Bridge Design Specifications*, California Department of Transportation, 2005, http://www.dot.ca.gov/manuals.htm, Accessed on March 19, 2005.

Campbell, I.M.C. and Weynberg, P.A., *Measurement of Parameters Affecting Slamming*, Final Report, Report No. 440, Technology Reports Centre No. OT-R-8042, Southampton University: Wofston Unit for Marine Technology, 1980.

CEM, 2006, *Coastal Engineering Manual*, U.S. Army Corps of Engineers, EM1110-2-1100, Accessed on 7-14-06, http://users.coastal.ufl.edu/~sheppard/eoc6430/Coastal_Engineering_Manual.htm.

Çengel Y. A., and Cimbala J. M., *Fluid Mechanics Fundamentals and Applications*, McGraw Hill, 2006.

Chan, E.S, Cheong H.F., and Gin, K.Y.H., *Breaking-Wave Loads on Vertical Walls Suspended Above Mean Sea Level*, Journal of Waterway, Port, Coastal, and Ocean Engineering, July/August, pp. 195-202, 1995.

Chen, W.F. and Duan, L., *Bridge Engineering Handbook*, (Eds.), CRC Press, 1999.

Denson, K.H., *Wave Forces on Causeway-Type Coastal Bridges*, Technical Report, Water Resources Research Institute, Mississippi State University, Project No. A-118-MISS, 1978.

Denson, K.H., *Wave Forces on Causeway-Type Coastal Bridges: Effects of Angle of Wave Incidence and Cross-Section Shape*, Water Resources Research Institute, Report No. MSHD-RD-80-070, Department of Civil Engineering, Mississippi State University, 1980.

Douglass, S.L., Chen, Q., Olsen, J.M., Edge, B.L., and Brown, D., *Wave Forces on Bridge Decks*, Draft Report, Prepared for the U.S. Department of Transportation, Federal Highway Administration, Office of Bridge Technology, Washington, D.C., April 2006, http://www.usouthal.edu/usacterec/waveforces.pdf, Accessed on July 20, 2006.

El Ghamry, O.A., *Wave Forces on a Dock*, Hydraulic Engineering Laboratory, Wave Research Projects, University of California, Berkeley, Institute of Engineering Research Technical Report HEL-9-1, 1963.

Faltinsen, O.M., *Sea Loads on Ships and Offshore Structures*, Cambridge Ocean Technology Series, Cambridge University Press, 1990.

FEMA, *Coastal Construction Manual*, Third Edition, Federal Emergency Management, CD, Vols. I, II, and III, June 2000.

FHWA, *Stream Stability at Highway Structures*, U.S., Federal Highway Administration, Hydraulic Engineering Circular No. 20, February 1991.

FHWA, *Evaluating Scour at Bridges*, U.S Department of Transportation, Federal Highway Administration, Hydraulic Engineering Circular No. 18, Fourth Edition, May 2001.

FHWA, *Tidal Hydrology, Hydraulics and Scour at Bridges*, U.S. Department of Transportation, Federal Highway Administration, Hydraulic Engineering Circular No. 25, Publication No. FHWA-NHI 04-077, December 2004.

Goda, Y., *A New Method of Wave Pressure Calculation for the Design of Composite Breakwater*, Proceedings 14th International Conference of Coastal Engineering, Copenhagen, pp. 1702-1720, 1974.

Goda, Y., *Random Seas and Design of Maritime Structures*, University of Tokyo Press, Tokyo, 1985.

Goda, Y., *Random Seas and Design of Maritime Structures*, Advanced Series on Ocean Engineering –Volume 15, Second Edition, World Scientific, 2000.

Hagiwara, K. and Yuhara, T., *Fundamental Study of Wave Impact Loads on Ship Bow*, Selected papers from the Journal of the Society of Naval Architecture, Japan, Vol. 14, pp. 73-85, 1976.

Hamill, L., *Bridge Hydraulics*, E and FN Spon (Routhledge), London, 1999.

Hedges, T.S., Proceedings of the Institution of Civil Engineers, Vol. 82, pp. 567-585, 1987.

Hinwood, J., *Design for Tsunamis Coastal Engineering Considerations*, Structural Engineering International, Vol. 3, pp. 189-193, 2005.

Issacson, M. and Prasad, S., *Wave Slamming on a Horizontal Circular Cylinder*, Proceedings, Civil Engineering in the Oceans V, R.T. Hudspeth, (Eds.), ASCE, Reston, VA, 1992.

Kaplan, P., *Wave Impact Forces on Offshore Structures: Re-Examination and New Interpretations*, 24th Annual Offshore Technology Conference, Houston, Texas, OTC 6814, May 4-7, pp. 79-86, 1992.

Kaplan, P., Murray, J.J., and Yu, W.C., *Theoretical Analysis of Wave Impact Forces on Platform Deck Structures*, Proceedings of the 14th International Conference on Offshore Mechanics and Arctic Engineering, American Society of Mechanical Engineers, Vol. 1-A, pp. 189-198, 1995.

Leira, B. and Langen, I., *On Probabilistic Design of a Concrete Floating Bridge*, Nordic Concrete Research, Vol. 3, pp. 140-166, December 1984.

Lwin, M., *Floating Bridges*, in Bridge Engineering Handbook, Chen, W.F. and Duan, L. (Eds.), CRC Press, 1999.

McConnell, K., Allsop, W., and Cruikshank, I., *Piers, Jetties and Related Structures, Exposed to Waves*, Guidelines for Hydraulic Loadings, HR Wallingford, Thomas Telford, 2004.

Minikin, R.R., *Winds, Waves and Maritime Structures*, Griffin, London, 1950.

Mitsuyasu, H., *Experimental Study on Wave Force Against a Wall*, Report Transportation Technical Research Institute, Ministry of Transport, Japan, Vol. 47, 1962.

NOAA/NGDC, http://www.ngdc.noaa.gov/seg/hazard/tsevsrch_idb.shtml, World Tsunami Database in text format, National Geophysical Data Center, U.S., Accessed on May 15, 2006.

Overbeek, J. and Klabbers, I.M., *Design of Jetty Decks for Extreme Vertical Wave Loads*, Proceedings of the Ports 2001 Conference, American Society of Civil Engineers, 10 pp., 2001.

Sarpkaya, T and Isaacson, M., *Mechanics of Wave Forces on Offshore Structures,* Van Nostrand Reinhold, 1981.

Shih, R.W. and Anastasiou, K., *Wave Induced Uplift Pressures Acting on a Horizontal Platform,* Presented at the Eighth International Conference on Offshore Mechanics and Arctic Engineering, March 19-23, The Hague, 1989.

SPM, Shore Protection Manual, Department of the Navy Waterways Experiment Station, Corps of Engineers, 1984.

Suchithra, N., and Koola, P.M., *A Study of Wave Impact on Horizontal Slabs*, Ocean Engineering, Vol. 22, No. 7, pp. 687-697, 1995.

Taly, N., *Design of Modern Highway Bridges*, McGraw Hill, 1998.

Tanimoto, K., *Wave Forces on a Composite-Type Breakwater*, Proceedings of the 1976 Annual Research Presentation of Port and Harbour Research Institute, pp. 1-26, 1976 (in Japanese).

Tedesco, J.W., McDougal, W.G., and Ross, C.A., *Structural Dynamics, Theory and Applications*, Addison Wesley, 1999.

Tickell, R.G., *Wave Forces on Structures*, Chapter 28, *Coastal, Estuarial and Harbour Engineer's Reference Book*, Abbott, M.B., and Price, W.A., (Eds.), Chapman and Hall, pp. 369-380, 1993.

TxDOT, *Bridge Design Manual*, http://manuals.dot.state.tx.us/docs/colbridg/forms/des.pdf, Accessed on March 18, 2005, Edition 2001.

TxDOT, *Hydraulic Design Manual*, Chapter 8 - Bridges, Texas Department of Transportation, January 1997.

Wang, H., *Water Wave Pressure on Horizontal Plate*, Journal of the Hydraulics Division, Proceedings of the American Society of Civil Engineers, Vol. 96, No. HY10, pp. 1997-2017, 1970.

Weggel, J.R., *Maximum Breaker Height for Design*, Proceedings 13th Coastal Engineering Conference, Vancouver, Vol. 1, pp. 419-432, 1972.

Weggel, J.R., *Discussion of Article: Breaking-Wave Loads on Vertical Walls Suspended Above Mean Sea Level*, Journal of Waterway, Port, Coastal, and Ocean Engineering, ASCE, May/June, pp. 143-147, 1997.

Wilson, J.F., *Dynamics of Offshore Structures*, Second Edition, John Wiley and Sons, 2003.

Xanthakos, P., *Bridge Substructure and Foundation Design*, Prentice Hall, 1995.